



## 저작자표시-비영리-변경금지 2.0 대한민국

이용자는 아래의 조건을 따르는 경우에 한하여 자유롭게

- 이 저작물을 복제, 배포, 전송, 전시, 공연 및 방송할 수 있습니다.

다음과 같은 조건을 따라야 합니다:



저작자표시. 귀하는 원저작자를 표시하여야 합니다.



비영리. 귀하는 이 저작물을 영리 목적으로 이용할 수 없습니다.



변경금지. 귀하는 이 저작물을 개작, 변형 또는 가공할 수 없습니다.

- 귀하는, 이 저작물의 재이용이나 배포의 경우, 이 저작물에 적용된 이용허락조건을 명확하게 나타내어야 합니다.
- 저작권자로부터 별도의 허가를 받으면 이러한 조건들은 적용되지 않습니다.

저작권법에 따른 이용자의 권리는 위의 내용에 의하여 영향을 받지 않습니다.

이것은 [이용허락규약\(Legal Code\)](#)을 이해하기 쉽게 요약한 것입니다.

[Disclaimer](#)

도시계획학 석사학위논문  
Analysis of vertical forest  
structure in Siheung  
with vegetation indices  
derived from LiDAR data

LiDAR 데이터를 이용한 식생 지수 개발과  
시흥시 산림 수직 구조 분석

2013 년 2 월

서울대학교 환경대학원

환경계획학과 환경관리전공

조 선

Analysis of vertical forest  
structure in Siheung  
with vegetation indices  
derived from LiDAR data

지도교수 이 도 원

이 논문을 도시계획학 석사 학위논문으로 제출함

2012 년 10 월

서울대학교 환경대학원

환경계획학과

조 선

조 선의 도시계획학 석사 학위论문을 인준함

2012 년 12 월

위 원 장 \_\_\_\_\_ (인)

부위원장 \_\_\_\_\_ (인)

위 원 \_\_\_\_\_ (인)

## **Abstract**

# **Analysis of vertical forest structure in Siheung with vegetation indices derived from LiDAR data**

Sun Cho

Department of Environmental Planning

Graduate School of Environmental Studies

Seoul National University

Remote sensing techniques have been developed to identify vegetation structure which affects the diversity and richness of wildlife as habitats. This study aims to develop the vegetation structure index which accurately illustrates the vertical structure of forests utilizing data derived from airborne LiDAR (Light Detection And Ranging), one of the emerging tool for surveying forest in remote sensing area with high accuracy and ability to identify the height of objects in the ground. The vertical structure of forest in the site Siheung is identified with utilizing non-ground returns of LiDAR data compared to the field survey data. The data treatment is classified in six layers, and percent cover of vegetation is estimated by density of LiDAR echoes. This showed distinct vertical structure between deciduous, coniferous and mixed forests in cover graph by layer. These metrics of

cover by layer were statistically verified by correlation analysis with layer data from field measurement and utilized to build vegetation structure indices. This study finds that a vegetation index on vertical structure with high accuracy is vertical evenness index, which identifies the evenness of vertical forest structure. This index shows the highest accuracy verified by referenced field data and differentiates three forest types: deciduous, coniferous and mixed forest. Due to the lack of high accuracy of GPS measurement in field survey and impeded detection of understory vegetation by LiDAR, the overall accuracy of LiDAR data was not as high as prediction from other studies. However, the limitation could be overcome by minimizing error on GPS and constructing models considering the Korean forest specific factors such as reflectance of native vegetation and topographic characteristics and this will be the base for the future study on the vertical structure of wildlife habitat in forest using discrete pulse airborne LiDAR.

keywords : vertical forest structure, vegetation index, airborne  
LiDAR, Siheung

*Student Number* : 2010-23897

## <Contents>

|   |           |
|---|-----------|
| <b>1. Introduction .....</b>                    | <b>1</b>  |
| <br><b>2. Material and Methods .....</b>        | <b>5</b>  |
| 2. 1. Theoretical background .....              | 5         |
| 2. 1. 1. Airborne LiDAR .....                   | 5         |
| 2. 1. 2. Vegetation structure and indices ..... | 7         |
| 2. 1. 3. LiDAR and vegetation structure .....   | 9         |
| 2. 2. Site description .....                    | 11        |
| 2. 3. Data collection .....                     | 14        |
| 2. 3. 1. Field measurements .....               | 13        |
| 2. 3. 2. LiDAR data extraction .....            | 21        |
| 2. 4. Data treatment .....                      | 23        |
| 2. 4. 1. Correlation analysis .....             | 23        |
| 2. 4. 2. Computed indices .....                 | 24        |
| <br><b>3. Results .....</b>                     | <b>35</b> |
| 3. 1. Descriptive statistics .....              | 35        |
| 3. 1. 1. Field data .....                       | 35        |
| 3. 1. 2. LiDAR data .....                       | 37        |

|  |           |
|--|-----------|
| 3. 1. 3. Cover graph by layers .....                   | 40        |
| 3. 2. Correlation analysis .....                       | 42        |
| 3. 2. 1. Cover by layers .....                         | 42        |
| 3. 2. 2. Combined cover layers .....                   | 44        |
| 3. 2. 3. Other metrics .....                           | 45        |
| 3. 3. Vegetation indices .....                         | 47        |
| 3. 3. 1. Vertical structure indices .....              | 47        |
| 3. 3. 2. Other indices .....                           | 51        |
| <b>4. Discussion .....</b>                             | <b>56</b> |
| 4. 1. Forest types and cover graphs by layers .....    | 56        |
| 4. 2. Correlation analysis of vegetation metrics ..... | 62        |
| 4. 3. Vegetation structure indices .....               | 65        |
| <b>5. Conclusions .....</b>                            | <b>69</b> |

## References

## Abstract (in Korean)

## <List of Table>

|  |    |
|--|----|
| <Table 2-1> Operating Parameters of LiDAR device which were employed in this study (Optech's ALTM 3070)  | 6  |
| <Table 2-2> Vegetation metrics derived from LiDAR data.  | 21 |
| <Table 2-3> Descriptive statistics of GPS errors. The first 6 sites do not have the record of error but they were not higher than 9 m.   | 22 |
| <Table 2-4> Vertical structure indices which were computed in this study using both site and LiDAR metrics.  | 31 |
| <Table 2-5> Tree species indices which were computed in this study using site metrics.   | 32 |
| <Table 2-6> Tree biomass indices which were computed in this study using site metrics.   | 33 |
| <Table 2-7> Vertical structure indices which were computed in this study using only LiDAR and site metrics, respectively.  | 34 |
| <Table 2-8> Vertical structure indices which were computed in this study using only LiDAR and site metrics, respectively.  | 34 |
| <Table 3-1> Descriptive statistics of the site data. Aspect and forest types are excluded as they are nominal scales.  | 35 |
| <Table 3-2> Descriptive statistics of the LiDAR derived data. The values of cvr, grnd, opn, std, and skw are excluded.   | 39 |
| <Table 3-3> The correlation coefficient of two proportion of cover data. The two height classes of layer 5 - 10 m and 10 - 20 m show significant correlation at the 0.01 level (2-tailed). | 43 |
| <Table 3-4> The names of combined layers and their height class, added layer metrics, Spearman's rho and R2 value.   | 44 |



|   |    |
|---|----|
| <Table 3-5> Correlation coefficient in Spearman's rho of other metrics from both site and LiDAR. The boxes with gray color indicate the correlation coefficients which are expected to have high correlation since the metrics quantify the same attributes.  | 46 |
| <Table 3-6> Correlation coefficients of Spearman's rho between vertical structure indices from LiDAR and site metrics.  | 50 |
| <Table 3-7> Correlation between tree species indices and vertical structure indices. Coefficients with bold text indicate the values over 0.600.  | 52 |
| <Table 3-8> Correlation coefficients of tree species indices  | 53 |
| <Table 3-9> Correlation coefficient in Spearman's rho between tree biomass indices and vertical structure indices.  | 54 |
| <Table 3-10> Correlation coefficient of HC index in Spearman's rho. Indices which does not have significant correlation coefficient is not listed in this table.  | 56 |
| <Table 4-1> The result of ANOVA using vegetation cover proportion of each layer to verify difference of mean of cover proportion by each layer. After Levene's test, Kruskal-Wallis test was used instead of ANOVA for the metrics which do not satisfy homoscedascity assumptions (layer0102, layer1020 and p_cvr_2000). | 58 |
| <Table 4-2> The proportion of genus composition in mixed forest plots.  | 59 |

## <List of Figures>

- <Figure 2-1> Google Earth satellite image of Siheung and adjacent cities with the layer indicating its administrative boundary 13
- <Figure 2-2> Biotope map of Siheung: regenerated deciduous forest (yellow), mixed forest (green), afforested deciduous forest (marine), afforested coniferous forest (brown), afforested mixed forest (purple) 14
- <Figure 2-3> Forest patches which have been managed by Forest tending service of the government (2009 - mid 2012) 16
- <Figure 2-4> Site points (●) with forest patches. The points are in the patches where the area has not been affected by the forest management of the local government. 17
- <Figure 2-5> Schematic picture of a quadrat 18
- <Figure 2-6> Schematic picture of transect measurement for percent cover of height classes. 20
- <Figure 2-7> Schematic picture of a quadrat and LiDAR circles. Three circles with radius 5 m, 7.0712 m, and 10 m, respectively and a quadrat colored with green. 23
- <Figure 3-1> Boxplot of percent cover in total 32 sites. 36
- <Figure 3-2> Boxplot of the proportion of percent cover in total 32 sites. 37
- <Figure 3-3> Boxplot of the proportion of percent cover by layers from LiDAR data in total 32 sites. 38
- <Figure 3-4> Cover graphs by layers. For the site graph, the proportion of cover is used and for LiDAR one, the data of layer is applied. The ordinates show the height of vertical structure in meter. 41

- <Figure 3-5> Scatter plots of two vegetation layer which shows the significant correlation coefficient by Spearman's rho at the 0.01 level (two-tailed). 43
- <Figure 3-6> Scatter plots of combined layers which have significant correlation coefficient by Spearman's rho at the 0.01 level (two-tailed). 45
- <Figure 3-7> Scatter plots of the metrics which show significant correlation with high coefficients. 46

# **1. Introduction**

Vegetation structure affects the diversity and richness of wildlife as habitats. Many studies have been conducted to find the relationship between vegetation structure and diversity of fauna which lives inside a forest (MacArthur and MacArthur, 1961, Karr, 1968, Roth, 1976, Ambuel & Temple, 1983, Buongiorno et al. 1994, Sullivan et al. 2001, Goetz et al. 2007). This relationship will give much advantageous information to protect endangered species by conserving their habitats in suitable structure. In order to implement conservation projects and research on the relationship of animal diversity and their habitats, it is crucial to identify the structure of vegetation for the animals which live inside it.

In addition to ecological or conservational objectives, the structure of vegetation has been one of the main research theme for the field of forest management as well. These days it became common to use sources from remote sensing such as satellite imagery and aerial photos to quantify the characteristics of forest like canopy height or to monitor forest in more efficient and effective ways. Compared to remote sensing technique, field measurement sometimes does not allow to carry on large scale investigation so it may be less efficient in

time and cost than remotely sensed way. However there are always issues of accuracy on utilizing remote sensing techniques since it requires verification with field measurement data, nor can it effectively figure out vertical element of vegetation structure.

Airborne LiDAR (Light Detection And Ranging) is one of remote sensing techniques which explore information of the earth with laser sensor loaded on aircraft. It makes it possible to enhance accuracy of methods which measure forest and its structure in an indirect way and identify the vertical structure of forest as well, which it makes high usage of study on forest structure. Since the sensor of LiDAR records the time gap of lasers which emit and return back in three coordinates with x, y, and z, this can be used to identify the vertical structure of objects or forest on terrain.

Using this characteristic of LiDAR, North American and European countries such as Canada, US and Germany try to utilize LiDAR data to extract accurate information on forest and to use it on forest management more frequently. Even LiDAR might be applied to researches in Korea not as much as other countries mentioned above, there are studies to utilize LiDAR data for determining quantitative properties of forest such as identifying forest structure, measuring canopy height and crown closure and estimating biomass of forest stand (Kim et al. 2010, Yoon et al. 2006, Lee et al. 2009).

However, in Korea, there are less researches utilizing LiDAR data

to investigate quantitative characteristic and structure of vegetation as habitats of wildlife and to contemplate them under the perspective of ecology. Ryu (2010) assessed habitat diversity in the scale of landscape and stand utilizing LiDAR data in order to suggest the way to improve biodiversity. Still the study utilizes LiDAR data with the purpose of biodiversity matters, it is less contemplative of the effect of forest structure to wildlife ecologically.

With perspective of identifying vertical structure of forest, Yoon and Lee (2000) tried to analyse structure of vegetation layers with Landsat imagery. The main purpose was not performing exact analysis of layered structure but the exploring techniques to analyse it with satellite source such as Landsat. It could be the first study which tried to utilize remote sensing data to identify the vertical or layered structure of vegetation but the results show different accuracy by each layer and do not illustrate the diversity of layered structure.

In this study, therefore, the vertical structure of forest in the site area is identified with utilizing non-ground returns of LiDAR data. The data treatment is further classified in six layers, and percent cover of vegetation is estimated by density of LiDAR echoes. With these metrics, a vegetation index on vertical structure with high accuracy is proposed, which later can be utilized to predict diversity of wildlife, especially avian communities, and elucidate diversity of the structure itself as well. Field measurement of sampled sites also

performed for statistical verification of the index.

The main and detailed questions of the study are as follows: (1) how accurate is information from LiDAR data on the vertical structure of vegetation?, and (2) which index would be the best and most effective in order to identify and illustrate the vertical structure of forest when using LiDAR data? In sum, the ultimate objective of this study is to develop the vegetation structure index which accurately illustrates the vertical structure of forests from airborne LiDAR data.

## **2. Material and Methods**

### **2. 1. Theoretical background**

#### **2. 1. 1. Airborne LiDAR**

The principle of LiDAR employs the methods using the time laser travels from sensor to objects in order to estimate the distance to the object. There are two ways of recording the time: pulse ranging and continuous wave ranging (Baltsavias, 1999). LiDAR is composed of GPS (Global Position System) which measures and records sensor and its location and IMU (Inertial Measurement Unit) which measures the orientation of the sensor (KIST, 2005).

In the case of pulse ranging type of airborne LiDAR, the laser pulse which injects from airborne sensor is reflected back by the object and the distance to the object can be calculated by the time which the laser pulse reflects back. This reflected pulse is called pulse or echo. It also has the information of the reflected point with x, y and z coordinates, which enable to build 3 dimensional information of terrain.

Using this characteristic, LiDAR is utilized to establish precise terrestrial information such as DEM (Digital Elevation Model) and to extract buildings and artificial structure when modeling a city. Also it



is used as a tool for managing forest because the mentioned characteristics of LiDAR provide data which enable to estimate species, canopy density, canopy height and even understory vegetation of forest. This information can also be processed to estimate crown closure and biomass of forest stands. Furthermore, this forest information can be utilized in the ecological species-habitat modeling as well (Vierling et al. 2008).

In this study, LiDAR data which had taken in January 2009 was analyzed. The data primarily collected by Hanjin Information Systems & Telecommunication Co. Ltd. employing Optech's ALTM 3070 of Canada. This machine acquires data using laser of scanning rate of 70kHz while flying 1200m altitude. The density of point is 3.5 per square meter (Table 2-1).

**Table 2-1** Operating Parameters of LiDAR device which were employed in this study (Optech's ALTM 3070)

|                     |                     |
|---------------------|---------------------|
| Date of acquisition | January 2009        |
| Collection altitude | 1200m               |
| Elevation accuracy  | 15 cm               |
| scanning rate       | 70kHz               |
| density of point    | 3.5 /m <sup>2</sup> |
| Range resolution    | 1 cm                |

## **2. 1. 2. Vegetation structure and indices**

Not only for forest management or study on forest ecosystem but also for biodiversity conservation, quantifying and indexing structure of forest has been conducted for a long time (Buongiorno et al. 1994, Sullivan et al. 2001). In South Korea, however, most studies on vertical structure of forest are conducted in the field, generally not employing remote sensing techniques and usually focus more on horizontal structure. However, there have been a large number of researches which tried to identify and model the forest structure in vertical direction in abroad.

Structural Complexity Index (SCI) established by Zenner and Hibbs (2000) is an index which is defined as the sum of the area of 3 dimensional triangle with x, y and z coordinates<sup>1)</sup>. It allows to compare the heterogeneity of stand structure and identify forest structure in 3 dimension. This index is based on the difference of components like diameter and the distance to neighboring trees. It suggests three dimensional structure which enables to model both horizontal and vertical structures, whereas one dimension index such as stem density, canopy cover and the number of canopy layer can be simply identified and two dimensional structure index explains horizontal structures such as location of individual trees.

---

1) X and Y are spatial coordinates and Z is dbh of trees.

Added to SCI, Zenner (2005) suggested structure-area-curves. This provides a useful tool to highlight scales when estimating differences of a stand type in the structural complexity and patch type variability. It also shows whether patch types and structural units have been mixed in the horizontal and vertical scales.

Neumann and Starlinger (2001) identified the correlation between species diversity of vegetation and structural diversity of stands using Shannon Index, Simpson Index, Evenness Index, Pielou Index and Cox Index. This research also developed a new index named Vertical Evenness (VE) with Shannon equation, which determines the characteristic of vertical structure in the stand scale. This calculates crown projection of four layers, the border of 80%, 50% and 20% from its highest tree height, and standardizes the result of four layers utilizing evenness formula (Table 2-4). Theoretical maximum value of vertical evenness is 1 and it means vertical evenly distributed tree within a stand.

In the early 1960's, MacArthur and MacArthur (1961) discovered that diversity of foliage or vertical arrangement of foliage has linear relationship with bird species diversity. They designed foliage height diversity (FHD), which describes the arrangement of foliage in different vertical layers with Shannon diversity index. The variable  $p_i$  in the equation indicates the proportion of total foliage of the  $i$ th

layer. Leaf area index was used to describe the foliage proportion in the study.

$$FHD = - \sum p_i \ln p_i$$

The result showed that the three height class of 0–0.61 m, 0.61–7.62 m, and over 7.62 m gave the best correlation with bird species diversity. Those classes correspond to the foliage layers of herbs, shrubs, and trees, respectively.

Ever since MacArthur and MacArthur (1961) designed FHD and showed tight correlation between foliage diversity and bird species diversity, there have been many researches which tried to identify the relationship between them, yet there are still critics on the study upon the subject of the standard method to measure foliage diversity and the arbitrariness of layer classes (McElhinny et al. 2005).

### **2. 1. 3. LiDAR and vegetation structure**

The attempt to identify diverse structure of forest and stand using LiDAR as a tool have been dramatically developed. The three dimensional coordinate system and high accuracy which make it possible to measure canopy height provide advantages to figure out vertical structure of vegetation. LiDAR is also employed to investigate three dimensional structure of forest as habitats for wildlife not just

for forest *per se*. Three dimensional arrangement of habitats provides fundamental information on how animals interact with environment (Vierlig et al. 2008).

As one of remote sensing techniques, LiDAR enables to approach in new ways surpassing existing labor-intensive measurement in the field and to explore more extensive areas within the same amount of time. It is highly evaluated that utilizing LiDAR data to identify wildlife and its habitats will be helpful to construct enhanced model for management and conservation of animal species (Verling et al. 2008).

Falkowski et al. (2009) determined successional characteristics of structurally diverse mixed forest with high accuracy of LiDAR for detecting vegetation structure. The study classified and modeled the three dimensional forest development in 6 stages and it showed accuracy higher than 95 percent.

Martinuzzi et al. (2009) utilized LiDAR data to map the presence/absence of snag diameter classes and understory shrub species. Using forest inventory plot, LiDAR measurement data and Random Forest algorithm (Breiman, 2001 cited in Martinuzzi et al. 2009), the achievement of its accuracy was as high as 83 percent for understory shrubs. Its performance was also proved by the case study of wildlife habitat suitability using four avian species. This study

detected not only the top canopy but also the presence of understory shrubs with high accuracy and used those LiDAR-derived metrics to assess quality of vegetation as bird habitats.

In this way, LiDAR has been used not only for forest management which seeks the way to utilize forest resources in effective way but also for forest ecology in terms of vegetation structure as wildlife habitat and forest succession. In this study, LiDAR data is applied to determine vegetation structure and density in forest plots as wildlife habitat for further researches such as wildlife habitat suitability of avifauna in temperate forests of Korea. Then LiDAR metrics are verified with field measurement and the accuracy was assessed with vegetation indexes.

## **2. 2. Site description**

Siheung is a city located near the south-western boundary of Seoul, the capital of South Korea. Seventy-one percent of its area used to be designated as part of the greenbelt zone of the capital for approximately 40 years. The restriction of development has been removed, yet the integrated and environmentally-friendly plans for urban development have not been settled (KICT, 2009). Therefore, it is important to identify the status of forest which had been restricted

to urban development since the forest serves as habitats for wildlife living inside the city and provide ecosystem services to people who reside in the city. Furthermore, researches on habitats of wildlife in the city have their own value, which allows to elucidate its connectivity in the metropolitan area, which links between the capital and satellite cities around it.

Therefore, this historical background as a former area of greenbelt zone and geographical location make Siheung a favorable research site for forest structure as wildlife habitat in terms of urban ecosystem service and forest connectivity of metropolitan area in South Korea. The whole area of the city has been scanned by LiDAR, which were funded by the local government and included every forest within the boundary of the city.

Also forest patches of Siheung are composed of deciduous, coniferous and mixed forests with the representative dominance genera of temperate forest in the central region of Korean peninsula: Genus *Quercus*, *Castanea*, *Pinus* and *Robinia*. These genera are either regenerated or afforested. These characteristics of the city make Siheung a perfect study site to fulfill the objective of this study within the context of Korean peninsula.

The total area of Siheung is approximately 135 km<sup>2</sup> and its area of green space is 39.1 km<sup>2</sup>, corresponding about 29% of the total area

(Siheung, 2011). Siheung faces the Yellow Sea in west so the forest patches in the city are mostly concentrated in the northern, eastern, and southeastern parts. These areas consist of mountains such as Mt. Sorae (north), Mt. Hakmi (north-west), Mt. Gunja (south) and Mt. Unheung (south-east) etc. Many patches especially in these mountains are connected to the adjoining Gyeonggi Province cities such as Gwangmyeong, Anyang, Gunpo, Ansan, and Incheon Metropolitan City. The terrestrial territory spans from 37°18'52"N to 37°28'18"N and from 126°41'67"E to 126°52'53"E approximately.



**Figure 2-1** Google Earth satellite image of Siheung and adjacent cities with the layer indicating its administrative boundary



## 2. 3. Data collection

### 2. 3. 1. Field measurements

#### 2. 3. 1. 1. Site sampling

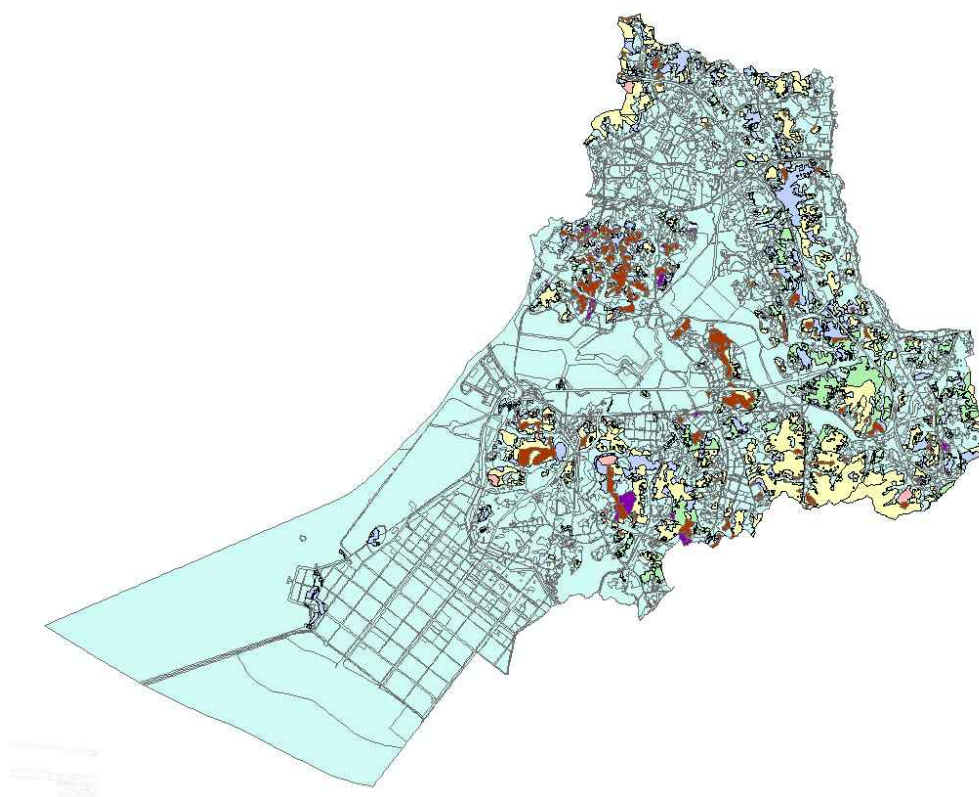


**Figure 2-2** Biotope map of Siheung: regenerated deciduous forest (yellow), mixed forest (green), afforested deciduous forest (marine), afforested coniferous forest (brown), afforested mixed forest (purple)

By the local government, silvicultural management practice in small scale is applied to forests in Siheung. The practice named “Forest Tending” is indicated in the Article 27 of the Creation and Management of Forest Resource Act and its Enforcement Decree and

Indications. This aims to manage forest to make it possible to grow healthier forest itself and to produce timbers in higher quality. By the age and status of a forest, management methods such as pruning, thinning and cultivating seedlings and small trees are selected and applied to each forest patch. Both regenerated and afforested forest patches are subject to the Act.

Conforming to the objectives of this study, the sampled sites should be the forest patches which have not been affected by the practice since January 2009 so that the LiDAR data could be as similar as possible to the sampled sites and show higher correlation with field data. In order to identify which forest patches have not been affected by the implementation of the Forest Tending service, the inventory of the forest addresses and the year of service implementation was assembled and joined to the GIS map. The inventory was provided by the local government officials in charge. Figure 2-3. shows the forest patches which have been managed by the local government since January 2009. These areas are marked in black color.

Sites were first sampled by the biotope type of forest: naturally regenerated deciduous forest, mixed forest, afforested deciduous forest, afforested coniferous forest, afforested mixed forest. As a forest patch which has not been managed was identified, the quadrat has been selected in accordance with the conditions followed: (1) the center of

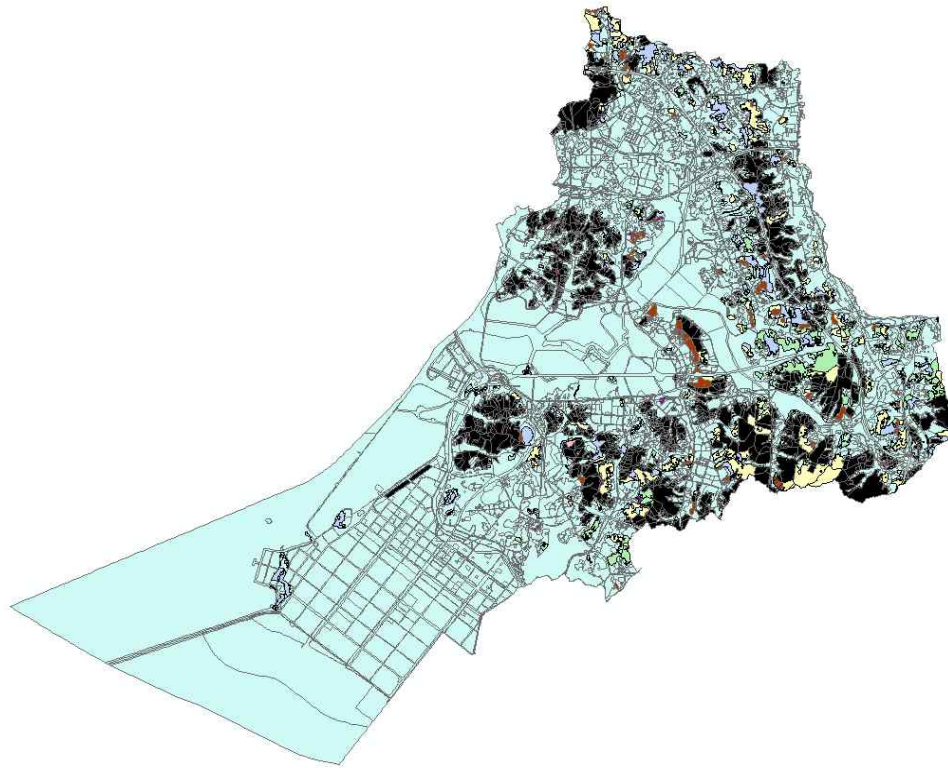


**Figure 2-3** Forest patches which have been managed by Forest tending service of the government (2009 - mid 2012)

the quadrat should be separated minimum 50 m from other biotope types in order to avoid edge effect and make the site close to interior patch, (2) the centers of quadrats should be separated minimum 200 m in order to reflect various forest patches inside Siheung city as many as possible. Figure 2-4. shows the total 32 sites in Siheung city with white circles (●); green areas are the forest patches. Field research was conducted from Sep. 12 to Oct. 20 2012, except for the first site which were measured on Jul. 31 2012.

### 2. 3. 1. 2. Quadrat method

In field research, the size of quadrat for woody plants is minimum 100 m<sup>2</sup> in flatland. As dominant trees make their distinct vertical structure by each species and community and affect growth and structure of other plants in a quadrat, their heights were measured by hypsometer (HaglofVertexLaser) to make them as precise as possible. In this study, tree height is especially critical since the metrics related

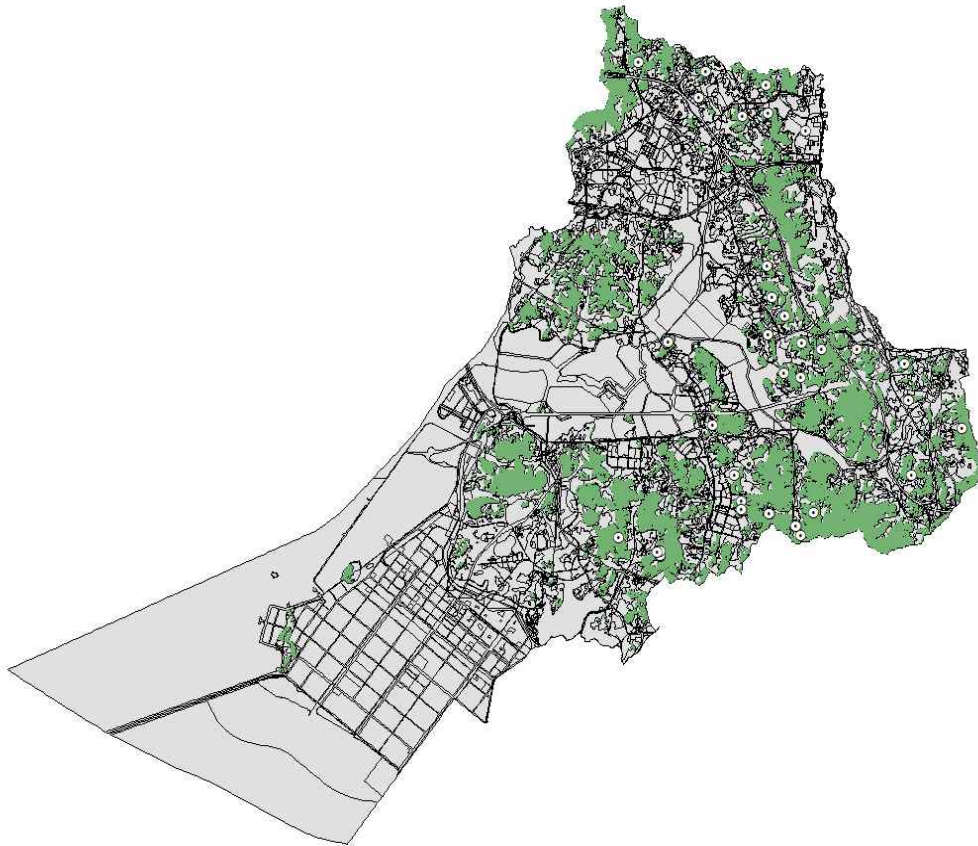


**Figure 2-4** Site points (⊙) with forest patches. The points are in the patches where the area has not been affected by the forest management of the local government.

to canopy height are built from LiDAR data such as maximum canopy height, mean canopy height, and standard deviation of the canopy height. These variables should be considered because these are directly linked to characteristics of vertical element of structure and standard deviation of tree height can be more indicative of vertical layers of foliage (McElhinny et al. 2005).

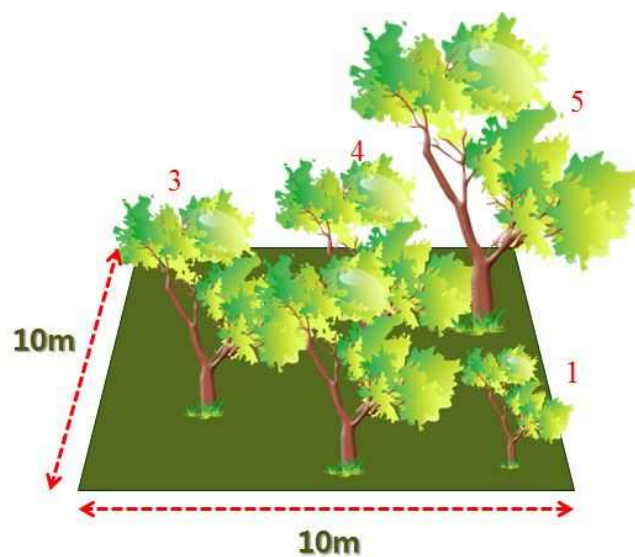


**Figure 2-5** Schematic picture of a quadrat

Dbh (diameter at breast height) of dominant trees was also measured with a dbh tape. Spies and Franklin (1991, cited from McElhinny et al. 2005) summarizes that dbh of Douglas-fir forest (i.e., metrics such as mean dbh, the standard deviation of dbh and the number of trees exceeding a threshold diameter) can be used for characterizing wildlife habitat, ecosystem function and successional development. Basal area, the sum of dbh in a quadrat, also can be

indicative of vegetation density, which shows approximate amount of vegetation of the whole part of tree (i.e., stem, branch, foliage, etc.).

Because a quadrat is to identify the dominant trees and to measure their dbh and height, only trees with dbh more than 5 cm are counted and measured. Moreover, even if there are shrubs which are higher than 2 m and might have dbh over 5 cm, those were not counted in a quadrat measurement. Although some Genus *Rhododendron* were taller than 3 m and their dbh are larger than 5 cm if all branches are added together, they were not precisely measured but surely affected distinctive presence of understory vegetation in transect measurement of percent cover.

#### 2. 3. 1. 3. Transect for percent cover

To measure percent cover by each height class (or layer) determining vertical structure of a quadrat, a perpendicular transect was applied inside a quadrat, modifying the methods exhibited in Helmer et al. (2000) and Schemske and Brokaw (1981). In the two coordinates of X and Y, two perpendicular transects which penetrate the center of a quadrat are drawn. Then, 5-meter staff with gradations is placed to measure the presence of vegetation in each height class.

The height was divided into 7 classes, which are expected to correspond to herb (0–1 m), shrub (1–2 m and 2–5 m) and trees

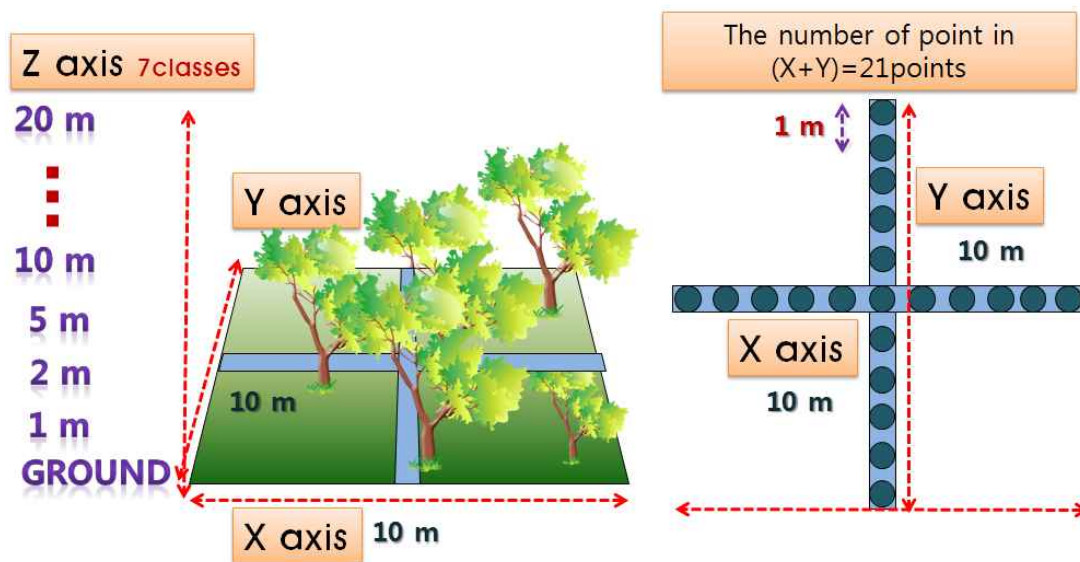


**Figure 2-6** Schematic picture of transect measurement for percent cover of height classes.

(over 5 m), respectively. Of higher than 5-meter class, trees were divided into 3 layers: 5–10 m, 10–20 m and over 20 m. This was devised to identify the vertical diversity of trees higher than 5m. Within 5 meter, if any vegetation including branches without foliage touches the vertical pole in one point in certain height class, it is recorded as the vegetation is present in the class. The vegetation presence of every class in all point in the transect, it is calculated as percent cover according to the simple equation below:

$$\text{Percent cover of one layer} = \frac{\text{The number of points where vegetation exists}}{\text{Total number of the points}}$$



### 2. 3. 2. LiDAR data extraction

The raw LiDAR data which was already classified into ground /non-ground returns by TerraScan and TerraModel of Terrasolid Ltd. processed by Hanjin Information Systems & Telecommunication Co.

**Table 2-2** Vegetation metrics derived from LiDAR data.

| Name      | Description   |
|-----------|---|
| layer0051 | Percentage of vegetation returns >0.5 m and ≤1m above ground (%)  |
| layer0102 | Percentage of vegetation returns >1 m and ≤2 m above ground (%)   |
| layer0205 | Percentage of vegetation returns >2 m and ≤5 m above ground (%)   |
| layer0510 | Percentage of vegetation returns >5 m and ≤10 m above ground (%)  |
| layer1020 | Percentage of vegetation returns >10 m and ≤20 m above ground (%) |
| layer2030 | Percentage of vegetation returns >20 m and ≤30 m above ground (%) |
| pnr0051   | Penetration ratio between 0.5-1 m above ground (%)                |
| pnr0102   | Penetration ratio between 1-2 m above ground (%)                  |
| pnr0205   | Penetration ratio between 2-5 m above ground (%)                  |
| pnr0510   | Penetration ratio between 5-10 m above ground (%)                 |
| pnr1020   | Penetration ratio between 10-20 m above ground (%)                |
| pnr2030   | Penetration ratio between 20-30 m above ground (%)                |
| cvr       | Canopy cover (Vegetation Returns >0.5 m /Total Returns (%))       |
| grnd      | Percentage of ground returns (Ground Returns/Total Returns (%))   |
| hmean     | Heights mean (m)  |
| h10       | Heights 10 <sup>th</sup> percentile (m)                           |
| h25       | Heights 25 <sup>th</sup> percentile (m)                           |
| h50       | Heights 50 <sup>th</sup> percentile (m)                           |
| h75       | Heights 75 <sup>th</sup> percentile (m)                           |
| h90       | Heights 90 <sup>th</sup> percentile (m)                           |
| hmax      | Maximum height (m)  |
| dtm       | Elevation (m)   |
| opn       | Openness below 2m from ground (Return < 2 m/Total Returns (%))    |
| std       | Standard deviation of the canopy height                           |
| skw       | Skewness of the canopy height                                     |



Ltd. are treated with *R* statistical package (R Development Core Team, 2011). Then, values of the metrics described in Table 2-2 were extracted.

Due to dense understory vegetation in some sites, GPS recorded the points of the bottom left corner of all quadrats, so the center points of each quadrat was later calculated from the GPS points of field sites. These estimated center points are then used to extract values of the LiDAR metrics. Since the quadrat is ideally a square with 10 m on a side, the distance between the bottom left corner and the center should be  $\frac{\sqrt{200}}{2}$  m, which is approximately 7.0712 m (easily applied as 7 m). Then, the error of GPS measurement (Table 2-3.) is also considered to extract values from LiDAR data. Finally 10 m radius circle is employed to calculate the values in each site. (See Figure 2-7).

**Table 2-3** Descriptive statistics of GPS errors. The first 6 sites do not have the record of error but they were not higher than 9 m.

| Variables          | Statistical values |
|--------------------|--------------------|
| Total Number       | 26                 |
| Maximum            | 9 m                |
| Minimum            | 4 m                |
| Mean               | 5.923 m            |
| Standard Deviation | 1.354 m            |

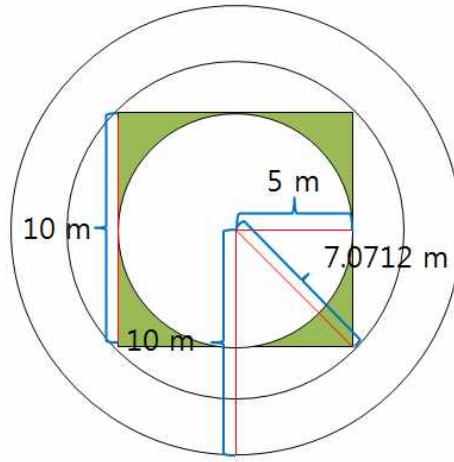


**Figure 2-7** Schematic picture of a quadrat and LiDAR circles. Three circles with radius 5 m, 7.0712 m, and 10 m, respectively and a quadrat colored with green.

After calculating the all values of LiDAR metrics from 5 m, 7 m and 10 m radius circle, the correlation between percent cover of field sites and layer values derived from LiDAR data showed the best with 10 m radius circle.

## 2. 4. Data treatment

### 2. 4. 1. Correlation analysis

To determine normality of data, the Shapiro-Wilk test is conducted for all data from the raw data of both field and LiDAR to the calculated values of indices with statistical software *R* package (R Development Core Team, 2011). Since several metrics do not have

significant p-values thus lack of normality, Spearman's rho is employed to analyse correlation between data using SPSS, version 20.0 (IBM Corp. 2011).

The correlation between percent cover of field and layer metrics of LiDAR was first analyzed to exclude outliers of data. The layer metrics from LiDAR means the proportion of each layer cover in a circular plot, so the percent cover values from field measurement are also transformed into proportion of each cover. This proportion data are inputted for correlation analysis with LiDAR data as a reference and also for Foliage Height Diversity calculation (For the details, see the next section upon indices.).

#### **2. 4. 2. Computed indices**

With the data from field and LiDAR, 17 indices were calculated. These indices refer to within-sample diversity (Neumann & Starlinger, 2001). Since LiDAR metrics only provide percent cover and data related to canopy height, except for the elevation, LiDAR data were utilized only for 6 indices which represent vertical structure of vegetation (Table 2-4).

As mentioned in the prior section, Foliage Height Diversity (FHD) was first proposed by MacArthur & MacArthur (1961). It originally utilizes the proportion of leaf area index for calculation with formula

of Shannon Index of Diversity. In this study, the proportion of vegetation cover of each layer is inputted into the formula. Higher value of FHD indicates higher diversity of vertical structure of vegetation in a plot.

Simpson Index of Diversity (Simpson, 1949) is also employed to estimate the diversity of vertical structure as following the same way which FHD utilizes Shannon Index. To make it have positive correlation, Simpson Index of Diversity instead of Simpson Index is applied since Simpson Index itself negatively correlates when the diversity of canopy layer increases. Therefore, higher value of FHD\_SimpID represents more diverse vertical structure.

Evenness Index (E) defines how the vegetation is evenly distributed in vertical structure. It employs the formula of Evenness Index of species. Instead of the value of Shannon Diversity of species, it uses that of vertical structure which could be interpreted as FHD since FHD is also derived from the Shannon formula. For denominator, it uses natural logarithm of the height class of trees.

Vertical Evenness (VE) is originally designed to characterize the vertical distribution of coverage within a stand when data of cover per layer is lacking. Instead of percent cover, Neumann & Starlinger (2001) first uses crown projection area of each layer with four relative height of 80, 50, 20% of maximum height in a plot, applying

to Shannon Index formula. For this study, VE is applied for 6 layer as itself and 4 layer to make the formula similar to the original one: 0–2 m, 2–10 m, 10–20 m, over 20m. The two VE with 6 layers and 4 layers were calculated by percent cover metrics both from field and LiADR. Also the formula applied to the height of certain percentile class derived from LiDAR data to make four classes of canopy. First it is utilized with *h10*, *h50*, *h90* and *hmax* and second, it employed height of 25, 50 75 and *hmax*, which makes the size of layers tend to be more even.

Coefficient of variation (CV) of canopy height shows the scatter of data and variability from the mean. When the value of CV is small, data scatter is small compared to the mean. With large CV value, it shows the amount of variation is large compared to the mean.

Height Class Richness shows the number of height classes occupied by trees. Higher value indicates more height classes which a stand occupies. However, this index does not consider relative abundance.

Other 10 indices use metrics from field measurement. These indices can be categorized into 3 major groups: (1) tree species indices (Table 2-5), (2) tree biomass indices (Table 2-6) and (3) combined index (Table 2-8, Neumann & Starlinger, 2001). Also another vertical structure indices is newly applied only to the field metrics: Margalef Diversity (Table 2-7).

Tree species indices quantify the diversity of vegetation in terms of its species, especially trees whose dbh is larger than 5 cm. Richness index represents the number of tree species in a 100 m<sup>2</sup> plot. The original Shannon Index of Diversity (Shannon, 1948) is employed to measure the diversity of tree species. With tree species, logarithm within the formula bases 2 instead of natural logarithms. Also the relative abundance was calculated by both basal area and the number of trees. The difference of these two relative abundances is discussed in the following sections.

Also Simpson Index of Diversity was also employed to measure species diversity of trees. This index also uses both basal area and the number of trees in a plot for the relative abundance. Evenness Index (Lloyd & Ghelardi, 1964; Magurran, 1988) also quantified the characteristics of tree species in a plot. By dividing the Shannon Index of Diversity by logarithm of the number of tree species, it shows how the tree species are evenly distributed within a plot.

With measured dbh of each tree whose size is larger than 5 cm of dbh, quadratic mean of dbh and basal area of unit area (100 m<sup>2</sup>) were able to be calculated. Compared to the arithmetic mean of dbh, the merit of quadratic mean of dbh is that it is directly related to stand basal area BA (m<sup>2</sup>ha<sup>-1</sup>) and the number of live trees in a unit area (ha<sup>-1</sup>) (McElhinny et al. 2006).

Also basal area of a plot is calculated employing the formula described in Table 2-6. The calculated basal area of a tree is then added up with all other trees in a plot. The index BA is resulted in a value with unit area ( $100\text{m}^2$ ), which represents tree biomass characteristic within a plot.

Since the species of tree and the number of trees are recorded when measuring dbh and tree height in the plots, the total number of stems in a plot was used as a simple index. Also CV of dbh is calculated. The details upon CV is already described in a paragraph above.

Due to the characteristics of metrics from LiDAR data, which mostly include ones related to canopy height and canopy cover, two vertical distribution indices were applied only with the LiDAR-derived metrics or with the field metrics. Goetz et al. (2007) developed Vertical Distribution Ratio (VDR) for full waveform LiDAR data to identify diversity of vertical structure and show its relationship with bird species richness. For application to discrete LiDAR pulse, the height of median energy (HOME) of the original formula ( $\text{VDR} = [\text{Canopy Height} - \text{HOME}] / \text{Canopy Height}$ ) is converted to  $h50$  (Heights 50th percentile (m)), one of the LiDAR metrics.  $hmax$  (For formula, see Table 2-7.) represents the maximum canopy height of a plot. VDR ranges between 0 and 1 and higher VDR value represents

areas of more even vertical distribution biomass whereas lower VDR, which means short distance between *hmax* and *h50*, indicates areas of a dense canopy with sparse understory vegetation (Goetz et al. 2007).

Margalef Diversity (Clifford and Stephenson, 1975) is a simple index mainly quantifying the range of tree height classes. Originally it was used for species richness index, but then this metrics related to height class can also be used to build index which characterizes height class of plots. However, this index is subject to the plot size but still straightforward and easy to be interpreted. When the number of height class increases, also does the index value. Because the formula of this index needs the term of total number of stem, the calculation for this index was only carried out with field metrics.

Complexity Index (HC) of Holdridge (1967) is the index which based on traditional measures of a stand. The value of index strongly is subject to the number of species and measures of growth performance and it does not contains information on spatial distribution. The index needs the measures of top height of trees, basal area, stem number and tree species, Neumann & Starlinger (2001) named it combined stand index.

Therefore, total 17 indices are employed in this study and the calculated values of indices are analyzed to figure out the correlation between LiDAR and field metrics, and among indices themselves as



well, which allows to figure out which index is the most efficient and powerful tool to identify forest structure and its characteristics.

**Table 2-4** Vertical structure indices which were computed in this study using both site and LiDAR metrics.

| Vertical structure indices   | Formula   | Description  |
|--|---|--|
| Foliage Height Diversity<br>with Shannon Diversity Index<br>(FHD_Sha, MacArthur & MacArthur, 1961)                   | $FHD_{Sha} = - \sum_i^n p_i \ln p_i$                    | $p_i$ is the proportion of vegetation cover in the $i^{\text{th}}$ height layer.   |
| Foliage Height Diversity<br>with Simpson Diversity Index<br>(FHD_SimpDI, MacArthur & MacArthur, 1961; Simpson, 1949) | $FHD_{Simp} = 1 - \sum_i^n p_i^2$                       | $p_i$ is the proportion of vegetation cover in the $i^{\text{th}}$ height layer.   |
| Evenness Index (EI, Pielou, 1975)  | $EI = \frac{FHD_{Sha}}{\ln N_h}$                        | $FHD_{Sha}$ is Shannon diversity calculated by the same formula of $FHD_{Sha}$ . $N_h$ is the number of height class occupied by tree heights. |
| Vertical Evenness<br>(VE, Neumann & Starlinger, 2001)  | $VE = \sum_i^4 (-\log p_i) \frac{p_i}{\log 4}$          | $p_i$ is the proportion of vegetation cover in the $i^{\text{th}}$ height layer.   |
| Coefficient of Variation<br>(CV, Sokal & Rohlf, 1981; Seavy et al. 2009)   | $CV_{ht} = \left( \frac{std}{hmean} \right) \times 100$ | $std$ is the standard deviation of canopy height. $hmean$ is the mean canopy height.   |
| Height Class Richness<br>(R, Fiala, 2003; Sullivan et al. 2001)  | $R = N_h$   | $N_h$ is the number of height classes occupied by trees.   |

**Table 2-5** Tree species indices which were computed in this study using site metrics.

| Tree species indices                                       | Formula                               | Description   |
|--|---------------------------------------|---|
| Richness Index (RI)  | $RI = N$                              | N is the number of tree species.  |
| Shannon Index of Diversity<br>(SH, Shannon, 1948)          | $SH = \sum_i^N (-\log_2 \pi_i) \pi_i$ | $\pi_i$ is the relative abundance of the $i^{\text{th}}$ species. This can be calculated by proportion of number, coverage or basal area. In this study, the number of trees and basal area are used as the relative abundance. |
| Simpson Index of Diversity<br>(SI, Simpson, 1949)          | $SI = \sum_i^N (1 - \pi_i) \pi_i$     | $\pi_i$ is the relative abundance of the $i^{\text{th}}$ species. This can be calculated by proportion of number, coverage or basal area. In this study, the number of trees and basal area are used as the relative abundance. |
| Evenness Index (E, Lloyd & Ghelardi, 1964; Magurran, 1988) | $E = \frac{SH}{\log_2 N}$             | SH is Shannon Index of Diversity and N is the number of species.  |

**Table 2-6** Tree biomass indices which were computed in this study using site metrics.

| Tree biomass indices  | Formula   | Description   |
|---|---|---|
| Quadratic mean dbh<br>(qdr_t_avg, McElhinny et al. 2006; Estes et al. 2010) | $DBH_q = \sqrt{\frac{\sum DBH^2}{n}}$                   | DBH is diameter of breast height of trees whose dbh >5 cm. n stands the stem number in a plot.  |
| Basal Area<br>(BA, Hédli et al. 2009)                                       | $BA(m^2) = 0.00007854 \times DBH^2$                     | DBH is diameter of breast height of trees whose dbh >5 cm. Later, BA of each tree in a plot is summed, which represents total BA in a unit area (100m <sup>2</sup> ). |
| Number of stem of trees   | $n$   | The total number of stem whose dbh >5 cm in a plot where the area is 100m <sup>2</sup> .  |
| Coefficient of Variation<br>(CV, Sokal & Rohlf, 1981)                       | $CV_{dbh} = \left(\frac{SD}{\bar{X}}\right) \times 100$ | SD is the standard deviation of dbh and $\bar{X}$ is the mean dbh of trees whose dbh >5 cm.   |

**Table 2-7** Vertical structure indices which were computed in this study using only LiDAR and site metrics, respectively.

| Vertical structure indices  | Formula                                  | Description   |
|---|--|---|
| Vertical Distribution Ratio<br>(VDR, Goetz et al. 2007)                 | $VDR = \frac{h_{max} - h_{50}}{h_{max}}$ | $h_{max}$ is the maximum canopy heights. $h_{50}$ is the heights 50 <sup>th</sup> percentile (m)  |
| Margalef Diversity (D <sub>mg</sub> ,<br>Clifford and Stephenson, 1975) | $D_{mg} = \frac{(N_h - 1)}{\ln n}$       | $N_h$ is the number of height classes occupied by tree heights. $n$ is either total number of stems or basal area per hectare for all height classes. |

**Table 2-8** Combined index which is computed in this study using site metrics.

| Combined index   | Formula                              | Description   |
|--|--------------------------------------|---|
| Complexity Index (HC,<br>Holdridge, 1967;<br>Neumann & Starlinger, 2001) | $HC = H \times BA \times n \times N$ | H is top-height, BA the basal area, n the stem number of trees which dbh >5 cm, N the number of tree species. |

### 3. Results

#### 3. 1. Descriptive statistics

##### 3. 1. 1. Field data

**Table 3-1** Descriptive statistics of the site data. Aspect and forest types are excluded as they are nominal scales.

| Metric Name | Minimum | Maximum | Average | Standard Deviation |
|-------------|---------|---------|---------|--------------------|
| cvr_0000    | 0.0000  | 0.2381  | 0.0450  | 0.0752             |
| cvr_0001    | 0.0435  | 0.9545  | 0.4393  | 0.2386             |
| cvr_0102    | 0.0000  | 0.7273  | 0.2860  | 0.1927             |
| cvr_0205    | 0.0909  | 1.0000  | 0.5212  | 0.2450             |
| cvr_0510    | 0.4091  | 1.0000  | 0.8785  | 0.1234             |
| cvr_1020    | 0.0870  | 1.0000  | 0.6388  | 0.2934             |
| cvr_2000    | 0.0000  | 0.5000  | 0.0883  | 0.1558             |
| p_cvr_0000  | 0.0000  | 0.0667  | 0.0148  | 0.0234             |
| p_cvr_0001  | 0.0169  | 0.3478  | 0.1504  | 0.0776             |
| p_cvr_0102  | 0.0000  | 0.1837  | 0.0934  | 0.0519             |
| p_cvr_0205  | 0.0250  | 0.3953  | 0.1832  | 0.0852             |
| p_cvr_0510  | 0.1915  | 0.4510  | 0.3161  | 0.0747             |
| p_cvr_1020  | 0.0435  | 0.3898  | 0.2164  | 0.0945             |
| p_cvr_2000  | 0.0000  | 0.1613  | 0.0257  | 0.0452             |
| hmax_s      | 12.8    | 29.6    | 18.4840 | 3.9010             |
| hmean_s     | 6.7846  | 17.6250 | 11.9490 | 2.5949             |
| dbh_max     | 22.9    | 79.7    | 34.8940 | 12.3197            |
| dbh_mean    | 11.4231 | 29.1500 | 18.5941 | 4.7785             |
| n           | 3       | 26      | 11.3438 | 5.3195             |
| RI          | 1       | 9       | 3.9100  | 1.8200             |
| slope_dg    | 5       | 32      | 19.91   | 5.986              |
| elevation   | 29      | 99      | 63.53   | 15.848             |

From field survey, total 9 metrics was calculated: percent cover of 7 vegetation layer, tree height, dbh, the number of tree species, the number of tree in a plot, forest type, aspect, slope and elevation. Percent cover is later transformed into the proportion of percent cover by layers (p\_cvr\_0000 - 2000) and utilized to calculate FHD and VE and correlation analysis with layer cover derived from LiDAR data.

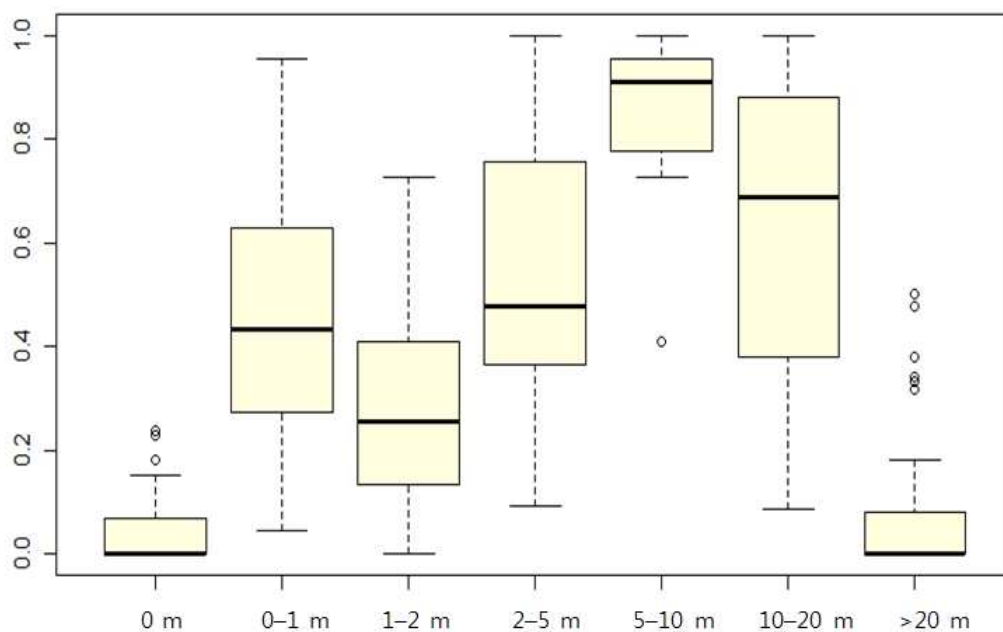


**Figure 3-1** Boxplot of percent cover in total 32 sites.

As shown in Figure 3-1 and 3-2, the boxplots of percent cover and its proportion are presented. In the lower layers of understory vegetation from ground to 5 meter, the value of percent cover is not as high as those of the higher layers (over 5 meter). This tendency also can be seen in the boxplot on its proportion. The average of the

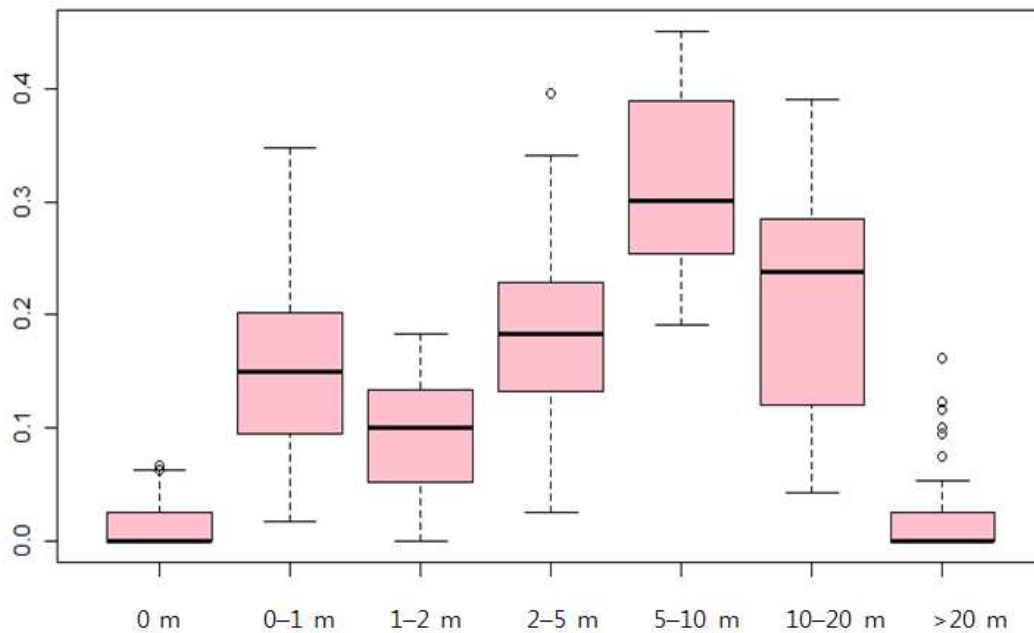


**Figure 3-2** Boxplot of the proportion of percent cover in total 32 sites.

highest layer class, layer over 20 m, is close to the value of zero, resulting from the fact that trees over 20 m height rarely exists in the study sites. The average age of forest in Korea is younger than other study sites in the US and the plots in forest patches are usually close to other biotope type, which makes the plot are likely to be exposed to other disturbance factors.

### 3. 1. 2. LiDAR data

Overall values of the proportion of percent cover from LiDAR data show slightly lower than those in field measurement. Especially, the understory vegetation below 5 m shows distinctively lower values.



This difference affects not only the result of correlation analysis of the metrics themselves but also the correlation of calculated vertical structure indices using this values. The details are described in the next chapter.

Also the layers over 5 m are different from data from site measurement. Layer 5 - 10 m shows the highest average of proportion in the field data but the data from LiDAR indicate that the average proportion of layer 5 - 10 m and 10 - 20 m is almost the same value while variance is higher in layer 10 - 20 m.

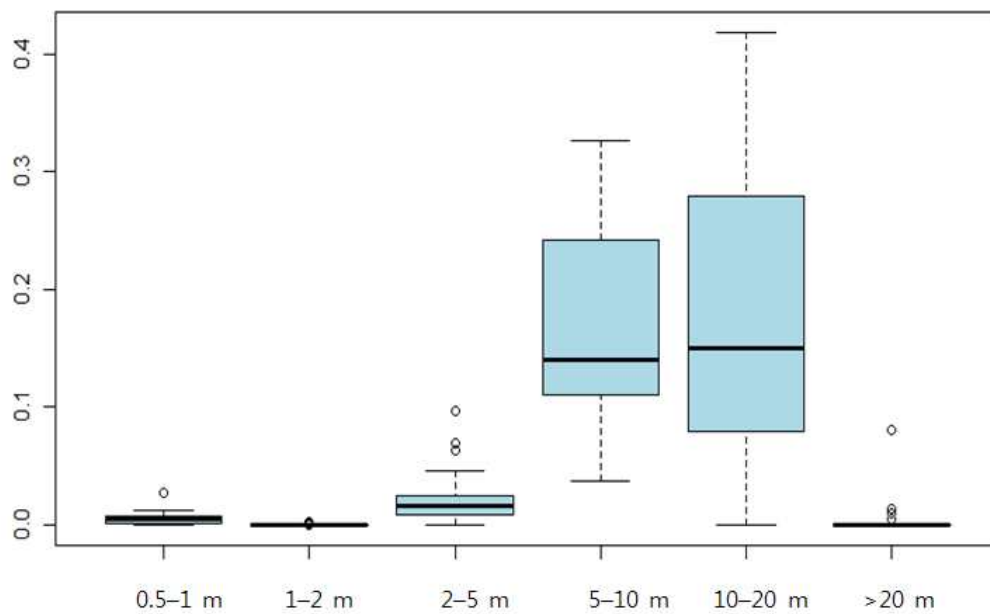


**Figure 3-3** Boxplot of the proportion of percent cover by layers from LiDAR data in total 32 sites.

The descriptive statistics of the LiDAR metrics are presented in Table 3-2. Layer 1 - 2 m has the smallest values compared to other layers, which almost converges on the value of zero and shows lower values than those of layer 0.5 - 1 m.

**Table 3-2** Descriptive statistics of the LiDAR derived data. The values of *cvr*, *grnd*, *opn*, *std*, and *skw* are excluded.

|           | Minimum | Maximum | Average | Standard<br>Deviation |
|-----------|---------|---------|---------|-----------------------|
| layer0051 | 0       | 0.0273  | 0.0053  | 0.0052                |
| layer0102 | 0       | 0.0020  | 0.0002  | 0.0004                |
| layer0205 | 0       | 0.0965  | 0.0224  | 0.0216                |
| layer0510 | 0.0375  | 0.3260  | 0.1705  | 0.0830                |
| layer1020 | 0       | 0.4185  | 0.1720  | 0.1192                |
| layer2030 | 0       | 0.0812  | 0.0036  | 0.0145                |
| pnr0051   | 0       | 0.0233  | 0.0070  | 0.0061                |
| pnr0102   | 0       | 0.0032  | 0.0003  | 0.0007                |
| pnr0205   | 0       | 0.0796  | 0.0232  | 0.0205                |
| pnr0510   | 0.0498  | 0.2508  | 0.1437  | 0.0536                |
| pnr1020   | 0       | 0.2963  | 0.1263  | 0.0860                |
| pnr2030   | 0       | 0.0666  | 0.0028  | 0.0118                |
| hmean     | 3.6052  | 9.8102  | 6.5439  | 1.5629                |
| h10       | 0.4385  | 5.7755  | 2.7685  | 1.3274                |
| h25       | 1.6189  | 7.3031  | 4.1972  | 1.5868                |
| h50       | 3.89    | 11.04   | 6.9282  | 1.76755               |
| h75       | 4.94    | 13.25   | 9.0344  | 2.0268                |
| h90       | 5.37    | 14.39   | 9.9984  | 2.29073               |
| hmax      | 5.66    | 15.09   | 10.6145 | 2.49339               |

The statistics of height metrics indicate that what LiDAR has detected is shorter and smaller trees in both average and maximum

values. Even if the time gap of three and half years between the data collection exists, it is considered that this resulted from the methods of measurement: LiDAR catches the values with several maximum points in average, while height measurement in the field directly counts the number and height of trees individually.

### **3. 1. 3. Cover graphs by layers**

The values of cover proportion by layer are drawn with the ordinates of vertical heights in meter, indicating the overall shape of vertical structure of forest. Field survey has measured the understory covers with higher accuracy in all forest types whereas LiDAR does not effectively detect vegetation cover in lower height classes, leading to no distinct peaks in the classes below 5 meter (Figure 3-4.).

The shape of cover graphs shows different vertical structure among three forest types. Deciduous forest draws a more rounded shapes in all height, indicating relatively abundant cover in most height class, especially higher strata such as layer higher than 10 m. On the other hand, coniferous forest shows a distinct and sharp peak in the layer 5 - 10 m, meaning that the vegetation density is highest in this layer and less dense in other layers. This can be interpreted as the typical crown shape of coniferous forests: conical shape of crown with less vegetation in understory.

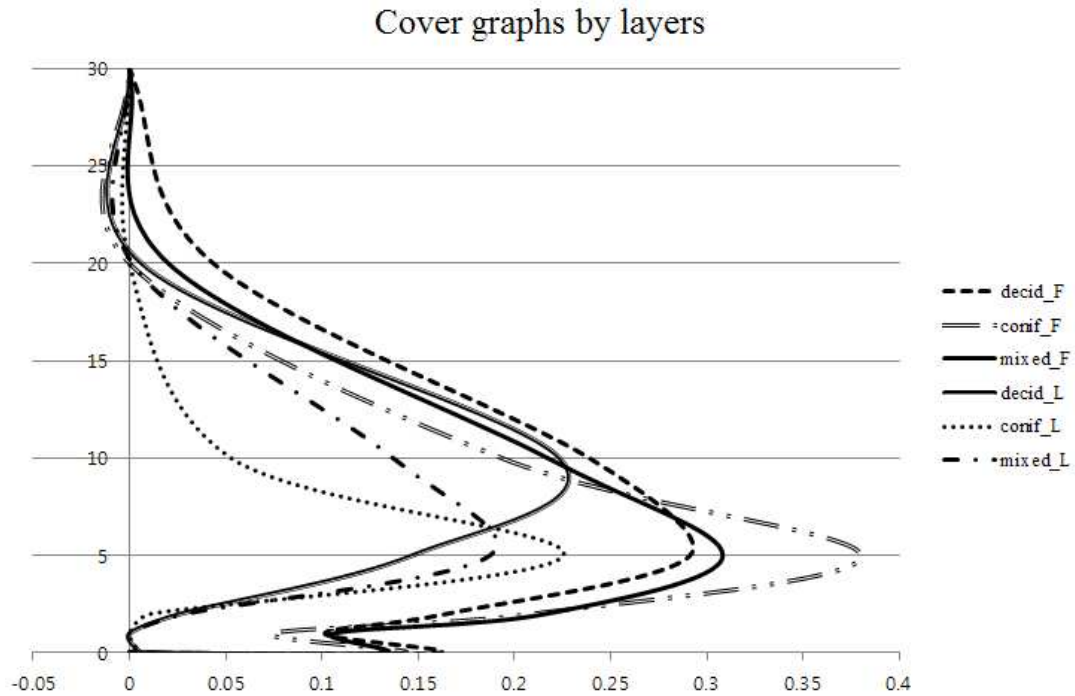


**Figure 3-4** Cover graphs by layers. For the site graph, the proportion of cover is used and for LiDAR one, the data of layer is applied. The ordinates show the height of vertical structure in meter

Aside coniferous forest which shows similar shapes in both site and LiDAR graphs, cover distribution shapes of deciduous and mixed forest draw different curves between field and LiDAR derived data. LiDAR curves distinguish the two different forest types by the peak, of which mixed forest is in lower height class than deciduous type. However, curves from field draw almost identical distribution shape. Especially in deciduous forest, the peaks of the two curves are located in different height class. The reason for this is considered in

later discussion section.

### **3. 2. Correlation analysis**

All correlation analysis of metrics and indices use the data only from 30 plots as two plots are determined as outliers (site No. 4 and 25, a deciduous plot and a coniferous one, respectively). Due to lack of normality in some layers and metrics, only Spearman's rho is indicated as correlation coefficient in the tables.

#### **3. 2. 1. Cover by layers**

To verify the accuracy of LiDAR-derived cover data, correlation analysis between layer covers from field and LiDAR data are conducted. As seen in Table 3-3, only two vegetation layer shows significance of correlation at the 0.01 level. Layer 5 - 10 m has the highest positive correlation between field and LiDAR data.

Lower height class below 2 m and the highest class of over 20 m show insignificant correlation coefficients. Since the vegetation cover of layer 1 -2 m has the smallest value, its correlation also shows the lowest coefficient. The scatter plots of two positively correlated layers are shown in Figure 3-5.

**Table 3-3** The correlation coefficient of two proportion of cover data. The two height classes of layer 5 – 10 m and 10 – 20 m show significant correlation at the 0.01 level (2-tailed).

|                     |            | LiDAR metrics (n=30) |           |           |           |           |           |
|---------------------|------------|----------------------|-----------|-----------|-----------|-----------|-----------|
|                     |            | layer0051            | layer0102 | layer0205 | layer0510 | layer1020 | layer2030 |
| Site metrics (n=30) | p_cvr_0001 | 0.227                |           |           |           |           |           |
|                     | p_cvr_0102 |                      | 0.19      |           |           |           |           |
|                     | p_cvr_0205 |                      |           | 0.313     |           |           |           |
|                     | p_cvr_0510 |                      |           |           | 0.638**   |           |           |
|                     | p_cvr_1020 |                      |           |           |           | 0.570**   |           |
|                     | p_cvr_2000 |                      |           |           |           |           | 0.154     |

\*\* Correlation is significant at the 0.01 level (2-tailed).

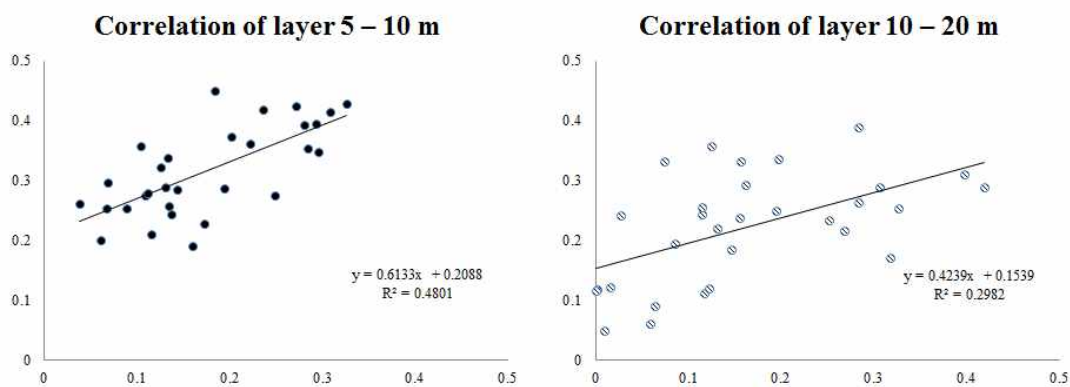


**Figure 3-5** Scatter plots of two vegetation layer which shows the significant correlation coefficient by Spearman's rho at the 0.01 level (two-tailed).

Since penetration ratio can be another indicative of the vegetation cover as described formula in Table 2-2, the correlation between proportion of cover from field plots and penetration ratio from LiDAR data was also analyzed. However, the result shows that correlation between layer cover is higher than that of the penetration ratio and

layer cover from fields (The result of correlation analysis is not displayed.).

### 3. 2. 2. Combined cover layers

Contrary to the expectation of high accuracy of LiDAR detection on percent cover in vegetation vertical structure, the correlation coefficient does not provide the precision of LiDAR when the metrics are

**Table 3-4** The names of combined layers and their height class, added layer metrics, Spearman's rho and R<sup>2</sup> value.

| Combined layer name | Height class   | Added layer metrics  | Spearman's rho | R <sup>2</sup> |
|---------------------|----------------|--|----------------|----------------|
| lyr_0005            | 0 - 5 m        | LiDAR: layer0051, 0102, 0205<br>Site: p_cvr_0001, 0201, 0205             | 0.054          | 0.0462         |
| lyr_0530            | 5 - over 20 m  | LiDAR: layer0510, 1020, 2030<br>Site: p_cvr_0510, 1020, 2000             | 0.328          | 0.0799         |
| lyr_0002            | 0 - 2 m        | LiDAR: layer0051, 0102<br>Site: p_cvr_0001, 0102                         | 0.195          | 0.0535         |
| lyr_0210            | 2 - 10 m       | LiDAR: layer0205, 0510<br>Site: p_cvr_0205, 0510                         | 0.594**        | 0.3329         |
| lyr_1030            | 10 - over 20 m | LiDAR: layer0510, 1020, 2030<br>Site: p_cvr_0510, 1020, 2000             | 0.594**        | 0.3307         |
| lyr_0220            | 2 - 20 m       | LiDAR: layer0205, 0510, 1020<br>Site: p_cvr_0205, 0510, 1020             | -0.084         | 0.0164         |
| lyr_0520            | 5 - 20 m       | LiDAR: layer0510, 0120<br>Site: p_cvr_0510, 0120                         | 0.339          | 0.0716         |
| lyr_0230            | 2 - over 20 m  | LiDAR: layer0205, 0510, 1020, 2030<br>Site: p_cvr_0205, 0510, 1020, 2000 | -0.139         | 0.0126         |

\*\* Correlation is significant at the 0.01 level (2-tailed).

verified with field ones. To improve correlation between data from two different sources, the value of each layer is combined and their correlation coefficients are analyzed again. As shown in Table 3-4, the results of the analysis show more original layers which correlates between site and LiDAR data. Even though the correlation coefficient itself is lower than that of layer 5 - 10 m alone, the combined layers with significant correlation coefficient at the 0.01 level now include layer 2 - 5 m and layer over 20 m, which do not show statistically significant correlation by the layers themselves. The scatter plots of these two combined layers are displayed in Figure 3-6.

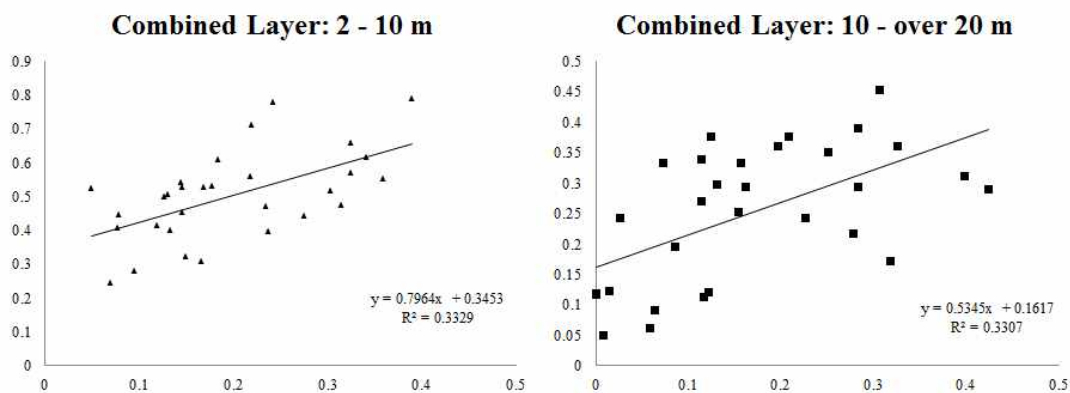


**Figure 3-6** Scatter plots of combined layers which have significant correlation coefficient by Spearman's rho at the 0.01 level (two-tailed).

### 3. 2. 3. Other metrics

The correlation of other metrics derived from LiDAR and measured from field plots also analyzed (Table 3-5). Total cover of a plot does



not significantly correlate, nor do the metrics such as *l-grnd* and *l-opn*. *l-grnd* and *l-opn* mean that subtracted value of *grnd* and *opn* from *l*, which can be used as surrogates of percent cover of a circular plot.

Even though maximum dbh correlates with total cover and skewness of canopy height distribution with low values of correlation coefficient, other metrics derived from field dbh measurement do not have significant correlation with other LiDAR-derived metrics.

**Table 3-5** Correlation coefficient in Spearman's rho of other metrics from both site and LiDAR. The boxes with gray color indicate the correlation coefficients which are expected to have high correlation since the metrics quantify the same attributes.

|                     |           | LiDAR metrics (n=30) |      |        |         |        |          |        |         |         |         |
|---------------------|-----------|----------------------|------|--------|---------|--------|----------|--------|---------|---------|---------|
|                     |           | cvr                  | grnd | l-grnd | hmax    | hmean  | std      | opn    | l-opn   | skw     | dtm     |
| Site metrics (n=30) | cvr_s_avg | -0.191               |      |        |         |        | 0.411*   |        |         |         |         |
|                     | cvr_s_sd  |                      |      |        |         |        |          |        |         |         |         |
|                     | p_cvr_sd  |                      |      |        | -0.455* |        | -0.544** |        |         | -0.361* |         |
|                     | ht_max    |                      |      |        | 0.723** | 0.434* | 0.717**  |        |         | 0.365*  |         |
|                     | ht_avg    |                      |      |        | 0.480** | 0.436* | 0.417*   |        |         |         |         |
|                     | ht_sd     | -0.413*              |      |        | 0.644** |        | 0.687**  | 0.434* | -0.434* |         |         |
|                     | dbh_max   | -0.384*              |      |        |         |        |          |        |         | 0.413*  |         |
|                     | dbh_avg   |                      |      |        |         |        |          |        |         |         |         |
|                     | dbh_sd    |                      |      |        |         |        |          |        |         |         |         |
|                     | dtm_s_m   |                      |      |        |         |        |          |        |         |         | 0.825** |

\* Correlation is significant at the 0.05 level (2-tailed).

\*\* Correlation is significant at the 0.01 level (2-tailed).

On the contrary the metrics from tree height measurement show very significant correlation with their corresponding ones. Their coefficient values are higher than those of layer 5 - 10 m (Spearman's rho: 0.638,  $p < 0.01$ ), which have the highest coefficient among height classes (For their scatter plots, see Figure 3-7).

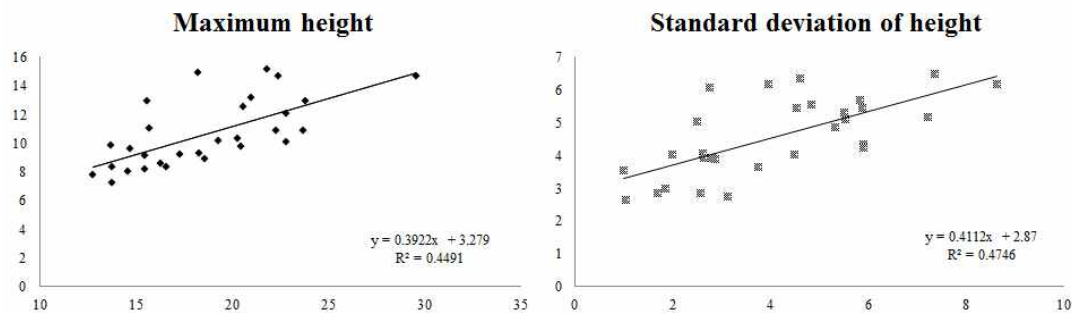


**Figure 3-7** Scatter plots of the metrics which show significant correlation with high coefficients.

The correlation of elevation of plots both from LiDAR and from field which was measured by GPS also provides high coefficient value. This result may be able to underpin the accuracy of GPS measurement in the field survey only if the process of obtaining elevation data from LiDAR and their values are reliable.

### 3. 3. Vegetation indices

#### 3. 3. 1. Vertical structure indices

Total 8 vertical structure indices are employed to identify which index

has the highest correlation between indices from LiDAR and field metrics (Table 3-6). Some indices are computed with different variables so have several results; these are presented with different tags at the end of index names.

VDR is applied only to LiDAR metrics because of the term  $h50$ , whereas Margalef Diversity is computed only by field metrics due to the term  $n$ , where  $n$  is the total basal area in a hectare or total number of trees in the stand, which cannot be directly derived from LiDAR data. Other 6 indices of vertical structure use the metrics both from field and LiDAR, whose accuracy can be easily determined by the value of correlation coefficient. Correlation analysis was applied not only to the same indices derived from different source but also to other vertical structure indices in order to evaluate the applicability of each index.

Some indices employed different variables into the same formula, which is labeled at the end of the index name. For example,  $lyr$  and  $n$  mean the number of height class (layer) and trees, respectively, and BH is basal area in a hectare. To calculating FHD, R and Margalef Diversity, the proportion of ground cover (0 m) is either included or excluded to see more suitable height classification since LiDAR-derived cover proportion has only 6 layers.

As seen in Table 3-6, VE with four layer classification shows the

highest correlation to itself and to other indices such as FHD, VDR, and R. VE is calculated in five other different ways and variables, but four layer classification of 0–2 m, 2–10 m, 10–20 m, over 20m with the data of proportion cover shows the highest performance in both field and LiDAR data.

**Table 3-6** Correlation coefficients of Spearman's rho between vertical structure indices from LiDAR and site metrics.

|  |                   |                | Vertical structure indices from LiDAR metrics |                         |         |         |                 |                 |                |                |         |         |         |        |
|--|-------------------|----------------|---|-------------------------|---------|---------|-----------------|-----------------|----------------|----------------|---------|---------|---------|--------|
|  |                   |                | FHD_Sh<br>a_6lyr                              | FHD_Si<br>mpID_6l<br>yr | VE_6lyr | VE_4lyr | VE_6lyr<br>_pnr | VE_4lyr<br>_pnr | VE_10p<br>c_ht | VE_25p<br>c_ht | VDR     | CV_ht   | R_6lyr  | E      |
| Vertical structure indices from site metrics | FHD_Sha_7lyr_s    | Spearman's rho | 0.306   |                         |         | 0.509** | 0.415*          | 0.505**         | 0.381*         |                | 0.560** | 0.436*  | 0.529** |        |
|  | FHD_Sha_6lyr_s    |                | 0.329   |                         |         | 0.499** | 0.389*          | 0.467**         |                |                | 0.577** | 0.499** | 0.513** |        |
|  | FHD_SimpID_7lyr_s |                |   | 0.217                   |         | 0.455*  |                 | 0.432*          |                |                | 0.487** | 0.382*  | 0.532** |        |
|  | FHD_SimpID_6lyr_s |                |   | 0.271                   |         | 0.438*  |                 | 0.402*          |                |                | 0.460*  | 0.397*  | 0.521** |        |
|  | VE_6yr_s          |                |   |                         | 0.331   | 0.499** | 0.389*          | 0.467**         |                |                | 0.577** | 0.499** | 0.513** |        |
|  | VE_4lyr_s         |                | 0.438*  |                         | 0.451*  | 0.683** | 0.506**         | 0.678**         | 0.548**        | 0.506**        | 0.513** | 0.419*  | 0.439*  |        |
|  | CV_ht_s           |                | 0.478**                                       |                         | 0.451*  | 0.453*  | 0.565**         | 0.532**         |                |                | 0.369*  | 0.443*  |         |        |
|  | R_7lyr_s          |                | 0.380*  |                         | 0.406*  | 0.520** | 0.483**         | 0.556**         | 0.468**        | 0.425*         | 0.488** |         | 0.456*  |        |
|  | R_6lyr_s          |                | 0.519**                                       |                         | 0.495** | 0.535** | 0.519**         | 0.527**         |                |                | 0.660** | 0.511** | 0.252   |        |
|  | Dmg_7lyr_n        |                |   |                         |         |         |                 | 0.392*          | 0.366*         |                | 0.513** |         |         | -0.207 |
|  | Dmg_7lyr_BA       |                |   |                         |         | 0.380*  | 0.365*          | 0.402*          | 0.402*         | 0.376*         | 0.511** |         | 0.437*  | -0.189 |
|  | Dmg_6lyr_n        |                |   |                         |         |         |                 | 0.361*          |                |                | 0.544** | 0.414*  |         | -0.143 |
|  | Dmg_6lyr_BA       |                |   |                         |         | 0.393*  | 0.409*          | 0.394*          |                |                | 0.712** | 0.552** |         | -0.055 |
|  | E_7lyr            |                |   |                         |         |         |                 |                 |                |                |         |         | 0.373*  | -0.199 |
| E_6lyr                                       |                   |                |   |                         |         |         |                 |                 |                |                | 0.436*  | -0.256  |         |        |

\* Correlation is significant at the 0.05 level (2-tailed).

\*\* Correlation is significant at the 0.01 level (2-tailed).

VDR is not able to be computed by field metrics, but it shows very high correlation with other indices from field metrics. The formula (Table 2-7) does not employ any height classification but still VDR correlates remarkably with the indices which utilizes the number of layers and layer classification. Also FHD shows good correlation with VE and VDR, but the index itself does not significantly correlate to FHD from LiDAR metrics.

### **3. 3. 2. Other indices from site metrics**

#### **3. 3. 2. 1. Tree species indices**

Four species indices are applied to the data from study plots. Input variables for these indices are the number of tree species, the relative abundance by basal area or the number of trees, which only can be acquired by field survey.

The correlation of tree species indices with the vertical structure indices was analyzed. There are some vertical structural indices which do not show any significant correlation coefficients to tree species indices<sup>2)</sup>. As shown in Table 3-7, FHD using Shannon formula with LiDAR metrics shows high correlation coefficients with tree species indices such as RI, SH and SI with the number of trees. Also VE

---

2) FHD\_SimpDI, VE\_10pc\_ht, VE\_25pc\_ht, R, E from LiDAR metrics and FHD\_SimpID\_7lyr\_s, FHD\_SimpID\_6lyr\_s, Dmg\_7lyr\_BA, Dmg\_7lyr\_n, E\_7lyr, E\_6lyr from field metrics

**Table 3-7** Correlation between tree species indices and vertical structure indices. Coefficients with bold text indicate the values over 0.600.

| Tree species indices from site metrics        |                |                |                |                |                |                |                |                |                |         |
|---|----------------|----------------|----------------|----------------|----------------|----------------|----------------|----------------|----------------|---------|
|   | Index name     |                | RI_s           | SH_BA_s        | SH_no_s        | SI_BA_s        | SI_n_s         | EI_SH_BA_s     | EI_SH_n_s      |         |
| Vertical structure indices from LiDAR metrics | FHD_Sha_6lyr   | Spearman's rho | <b>0.722**</b> | 0.451*         | <b>0.698**</b> | 0.424*         | <b>0.684**</b> |                | 0.534**        |         |
|   | VE_6lyr        |                | <b>0.677**</b> | 0.437*         | <b>0.672**</b> | 0.424*         | <b>0.666**</b> |                | 0.540**        |         |
|   | VE_4lyr        |                | 0.492**        |                | 0.538**        |                | 0.566**        |                | 0.468**        |         |
|   | VE_6lyr_pnr    |                | <b>0.678**</b> | 0.438*         | <b>0.726**</b> | 0.431*         | <b>0.737**</b> |                | <b>0.618**</b> |         |
|   | VE_4lyr_pnr    |                | 0.496**        |                | 0.587**        |                | <b>0.626**</b> |                | 0.549**        |         |
|   | VDR            |                | 0.362*         |                | 0.464**        |                | 0.518**        |                | 0.553**        |         |
|   | CV_ht          |                | 0.422*         | 0.401*         | 0.490**        | 0.382*         | 0.527**        |                | 0.511**        |         |
| Vertical structure indices from site metrics  | FHD_Sha_7lyr_s |                |                |                |                |                |                | 0.369*         |                |         |
|   | FHD_Sha_6lyr_s |                |                |                | 0.374*         | 0.400*         |                | 0.446*         |                | 0.406*  |
|   | VE_6lyrs_s     |                |                |                | 0.374*         | 0.400*         |                | 0.446*         |                | 0.406*  |
|   | VE_4lyrs_s     |                |                | 0.383*         | 0.450*         | 0.470**        | 0.425*         | 0.535**        | 0.376*         | 0.515** |
|   | CV_ht_s        |                |                | <b>0.648**</b> |                | <b>0.607**</b> |                | <b>0.602**</b> |                | 0.392*  |
|   | R_7lyr_s       |                |                |                |                |                |                | 0.381*         |                |         |
|   | R_6lyr_s       |                |                | 0.512**        | 0.429*         | 0.578**        | 0.362*         | <b>0.614**</b> |                | 0.531** |
|   | Dmg_6lyr_n     |                |                |                |                |                |                |                | 0.387*         |         |
|   | Dmg_6lyr_BA    |                |                | 0.364*         | 0.411*         |                | 0.467**        |                | 0.457*         |         |

\* Correlation is significant at the 0.05 level (2-tailed).

\*\* Correlation is significant at the 0.01 level (2-tailed).

with 6 layers shows high correlation coefficients. Compared to LiDAR indices, field indices of vertical structure show lower coefficient values than those of LiDAR. FHD with Shannon formula does not have good correlation as vertical structure index itself, but FHD<sub>Sha</sub> derived from LiDAR data is likely to be a good predictor of tree species indices like RI, SH and SI with the number of trees. It may be said that FHD derived from LiDAR data has higher ability to

underpin the tendency of tree diversity and richness rather than species evenness of trees in a plot.

Tree species indices like SH, SI and EI are calculated by two different variables: proportion of basal area by tree species (BA) and the number of tree species (n). The correlation analysis between these indices themselves are conducted and the results are shown in Table 3-8. Even though the identical tree species indices employing different variables have very high correlation (i.e. SH\_BA vs. SH\_n and

**Table 3-8** Correlation coefficients of tree species indices

|          |                | RI_s    | SH_BA   | SH_n    | SI_BA   | SI_n    | EI_SH_<br>BA | EI_SH_n |
|----------|----------------|---------|---------|---------|---------|---------|--------------|---------|
| RI_s     | Spearman's rho | 1       |         |         |         |         |              |         |
| SH_BA    |                | 0.754** | 1       |         |         |         |              |         |
| SH_n     |                | 0.946** | 0.821** | 1       |         |         |              |         |
| SI_BA    |                | 0.698** | 0.985** | 0.780** | 1       |         |              |         |
| SI_n     |                | 0.899** | 0.818** | 0.987** | 0.779** | 1       |              |         |
| EI_SH_BA |                | 0.272   | 0.775** | 0.393*  | 0.816** | 0.423*  | 1            |         |
| EI_SH_n  |                | 0.699** | 0.778** | 0.873** | 0.768** | 0.908** | 0.558**      | 1       |

\* Correlation is significant at the 0.05 level (2-tailed).

\*\* Correlation is significant at the 0.01 level (2-tailed).

SI\_BA vs. SI\_n) but the correlation of these tree species indices with vertical structure indices indicate different coefficient values. For example, SH\_BA and SH\_n are significantly correlated at the level of 0.01 with the coefficient of 0.821 (Table 3-8). However, most LiDAR-derived vertical structure indices and CV\_ht\_s from field show



higher values of correlation coefficient in the tree species indices calculated with the variable ‘the number of trees (n)’.

### 3. 3. 2. 2. Tree biomass indices

**Table 3-9** Correlation coefficient in Spearman’s rho between tree biomass indices and vertical structure indices.

|   |              | Tree biomass indices from site metrics |         |   |        |
|---|--------------|--|---------|---|--------|
|   |              | qdr_t_avg                              | CV_dbh  | n | BA     |
| Vertical structure indices from LiDAR metrics | FHD_Sha_6lyr |  | 0.604** |   |        |
|   | VE_6lyr      |  | 0.558** |   |        |
|   | VE_4lyr      |  | 0.445*  |   |        |
|   | VE_6lyr_pnr  |  | 0.572** |   |        |
|   | VE_4lyr_pnr  |  | 0.458*  |   |        |
|   | CV_ht        |  | 0.419*  |   |        |
| Vertical structure indices from site metrics  | E            |  | 0.492** |   | 0.378* |
|   | CV_ht_s      |  | 0.805** |   |        |
|   | R_6lyr_s     |  | 0.377*  |   |        |

\* Correlation is significant at the 0.05 level (2-tailed).

\*\* Correlation is significant at the 0.01 level (2-tailed).

Four tree biomass indices were calculated and analyzed for correlation with other indices. Many vertical structural indices do not show any significant correlation coefficients, which are excluded in the result (Table 3-9). Especially the formula of Margalef Diversity index

includes the term ‘total number of stem’ or those derived from it. Therefore, this index is excluded in the correlation result with tree biomass indices, even though it shows significant correlation coefficient with indices  $n$  and  $BA$ . As shown in Table 3-9, only  $CV\_dbh$  has significant correlation with vertical structure indices and  $BA$  weakly correlates only with  $E$  from LiDAR metrics.

### 3. 3. 2. 3. Combined index: HC

HC is a complexity index (Holdridge, 1967) which is rather based on traditional measures of stand and does not explain much about spatial distribution or within stand variation (Neumann & Starlinger, 2001). As seen in the formula within Table 2-8, this index strongly affected by the number of species and growth performance measurement. The correlation of HC with other indices are analyzed; various indices in all three categories of vertical structure indices, tree biomass indices and tree species indices correlates with HC. This is because HC is computed with the average of three highest trees, basal area, the number of trees and the number of species.

**Table 3-10** Correlation coefficient of HC index in Spearman's rho. Indices which does not have significant correlation coefficient is not listed in this table.

|  |              | HC      |
|--|--------------|---------|
| Vertical distribution indices from site metrics  | CV_ht_s      | 0.558** |
|  | D_7lyr_N     | -0.426* |
|  | D_6lyr_N     | -0.419* |
| Vertical distribution indices from LiDAR metrics | FHD_Sha_6lyr | 0.639** |
|  | VE_6lyr      | 0.586** |
|  | VE_4lyr      | 0.374*  |
|  | VE_6lyr_pnr  | 0.514** |
|  | VE_4lyr_pnr  | 0.378*  |
|  | E            | 0.489** |
| Tree biomass indices                             | CV_dbh       | 0.639** |
|  | n            | 0.708** |
|  | BA           | 0.666** |
| Tree species indices                             | RI_s         | 0.805** |
|  | SH_BA        | 0.429*  |
|  | SH_n         | 0.667** |
|  | SI_BA        | 0.388*  |
|  | SI_n         | 0.610** |
|  | EI_SH_n      | 0.373*  |

\* Correlation is significant at the 0.05 level (2-tailed).

\*\* Correlation is significant at the 0.01 level (2-tailed).

## **4. Discussion**

### **4. 1. Forest types and cover graphs by layers**

According to cover graphs in Figure 3-4, tree height distribution and its vertical structure are fairly different among forest types. Field survey curves indicate that the understory of coniferous forest within the layer of 1–2 m shows lower proportion of vegetation cover than deciduous or mixed forest but this could not be verified statistically. (Table 4-1).

Only 5–10 m layer from field survey and 10–20 m one from LiDAR data statistically proved significantly different vegetation cover among forest types. By Tukey's method, it was identified that the between-group differences were from deciduous and coniferous forest: p-value for p\_cvr\_0510 was 0.023 ( $p < 0.05$ ) and that for layer of 10 – 20 m was 0.002 ( $p < 0.01$ ). This results can be the statistical grounds for the reason on the different layer classes where the peaks of curves placed in Figure 3-4. Field measurement curve of cover by layer depicts the dense vegetation of conifers in the 5–10 m layer with relatively sharp peak. LiDAR derived cover draws different peak between deciduous and coniferous forest. The peak of deciduous forest is located in the layer of 10–20 m and it would make considerable differences in vegetation density and so does in proportion of cover

**Table 4-1** The result of ANOVA using vegetation cover proportion of each layer to verify difference of mean of cover proportion by each layer. After Levene's test, Kruskal-Wallis test was used instead of ANOVA for the metrics which do not satisfy homoscedascity assumptions (layer0102, layer1020 and p\_cvr\_2000).

|            |                            | Sum Sq. | df | Mean Sq. | F value | p-value |
|------------|----------------------------|---------|----|----------|---------|---------|
| layer0051  | Between-group              | 0       | 2  | 0        | 0.225   | 0.800   |
|            | Within-group               | 0.001   | 27 | 0        |         |         |
|            | Total                      | 0.001   | 29 |          |         |         |
| p_cvr_0001 | Between-group              | 0.004   | 2  | 0.002    | 0.278   | 0.760   |
|            | Within-group               | 0.171   | 27 | 0.006    |         |         |
|            | Total                      | 0.174   | 29 |          |         |         |
| layer0102  | Kruskal-Wallis chi-squared | 2.418   | 2  |          |         | 0.298   |
| p_cvr_0102 | Between-group              | 0.004   | 2  | 0.002    | 0.761   | 0.477   |
|            | Within-group               | 0.075   | 27 | 0.003    |         |         |
|            | Total                      | 0.08    | 29 |          |         |         |
| layer0205  | Between-group              | 0.001   | 2  | 0.001    | 1.569   | 0.227   |
|            | Within-group               | 0.012   | 27 | 0        |         |         |
|            | Total                      | 0.014   | 29 |          |         |         |
| p_cvr_0205 | Between-group              | 0.018   | 2  | 0.009    | 1.17    | 0.326   |
|            | Within-group               | 0.206   | 27 | 0.008    |         |         |
|            | Total                      | 0.224   | 29 |          |         |         |
| layer0510  | Between-group              | 0.031   | 2  | 0.016    | 2.461   | 0.104   |
|            | Within-group               | 0.172   | 27 | 0.006    |         |         |
|            | Total                      | 0.204   | 29 |          |         |         |
| p_cvr_0510 | Between-group              | 0.037   | 2  | 0.019    | 4.013   | 0.030*  |
|            | Within-group               | 0.125   | 27 | 0.005    |         |         |
|            | Total                      | 0.162   | 29 |          |         |         |
| layer1020  | Kruskal-Wallis chi-squared | 10.825  | 2  |          |         | 0.004** |
| p_cvr_1020 | Between-group              | 0.009   | 2  | 0.005    | 0.53    | 0.595   |
|            | Within-group               | 0.233   | 27 | 0.009    |         |         |
|            | Total                      | 0.243   | 29 |          |         |         |
| layer2030  | Between-group              | 0       | 2  | 0        | 0.519   | 0.601   |
|            | Within-group               | 0.006   | 27 | 0        |         |         |
|            | Total                      | 0.007   | 29 |          |         |         |
| p_cvr_2000 | Kruskal-Wallis chi-squared | 5.562   | 2  |          |         | 0.062   |

\*  $p < 0.05$ , \*\*  $p < 0.01$

whereas the pointed peak of conifer lies in the layer of 5–10 m.

Figure 3-4 distinctly depicts the difference of vertical vegetation cover between coniferous and deciduous/mixed forest by both field and LiDAR data. The sharp peak of conifers would illustrate the conical shape of their species such as *Pinus koraiensis*. Also, this is statistically underpinned by the ANOVA results (Table 4-1).

However, the curves of deciduous and mixed forest from field metrics show similar patterns. The reason considered is that mixed forests of the plots in Siheung are slightly more dominated by deciduous genera *Quercus* and *Castanea*, mixed-deciduous forest comprising 67.47 % of the whole trees in a mixed forest plot (Table 4-2), so vertical distribution of mixed forest would show similar pattern to that of deciduous forest.

**Table 4-2** The proportion of genus composition in mixed forest plots.

| Site No. | No. of trees | % of deciduous trees | % of <i>Quercus</i> | % of <i>Castanea</i> | % of <i>Robinea</i> | % of others | % of conifers |
|----------|--------------|----------------------|---------------------|----------------------|---------------------|-------------|---------------|
| 10       | 10           | 70.00                | 70.00               | 0.00                 | 0.00                | 0.00        | 30.00         |
| 11       | 15           | 86.67                | 20.00               | 13.33                | 26.67               | 26.67       | 13.33         |
| 20       | 10           | 90.00                | 60.00               | 30.00                | 0.00                | 0.00        | 10.00         |
| 23       | 11           | 45.45                | 36.36               | 0.00                 | 0.00                | 9.09        | 54.55         |
| 24       | 16           | 31.25                | 12.50               | 12.50                | 6.25                | 0.00        | 68.75         |
| 27       | 4            | 75.00                | 0.00                | 75.00                | 0.00                | 0.00        | 25.00         |
| 28       | 17           | 82.35                | 35.29               | 5.88                 | 29.41               | 11.76       | 17.65         |
| Total    | 83           | 67.47                | 33.73               | 13.25                | 12.05               | 8.43        | 32.53         |
| Mean     | 11.86        | 68.67                | 33.45               | 19.53                | 8.90                | 6.79        | 31.33         |

On the other hand, the curve pattern of mixed forest from LiDAR metrics has its own distinctive shape: the peak of its curve is located in the lower layer compared to deciduous forest, yet the shape of peak is not as sharp as coniferous one and the curve shows higher vegetation density in higher strata such as over 10 m compared to the curve of conifers. Why the mixed forest has its own distinguishable curve shape though the curves of deciduous and mixed forest from field measurement are nearly identical? The difference in the plot radius could cause this distinction between curves of mixed forest from field and LiDAR data.

Considering the measurement error of GPS and the nature of plot shape, LiDAR variables extracted with a radius of 10 m whereas the length of a quadrat's side was normally 10 m. This made the size of a quadrat smaller than that of a circular sampling site of LiDAR (See Figure 2-7 for the details.). When the forest type is categorized, the characteristics and type of the surrounding forest areas were taken into account. Field sites such as 11, 20 and 28 has less conifer trees within each quadrat but there were definitely more coniferous trees around quadrats, which make them considered as a mixed forest plot. Therefore, the curve from LiDAR on mixed forest would have a distinct shape and can be easily distinguishable from the cover, whereas that from field survey has rather identical shape with

deciduous one.

Even though the curves of mixed forest have similar patterns with deciduous forest's ones both by field and LiDAR, the curve of deciduous forest from LiDAR data depicts its distinct characteristic: its peak lies in higher strata than that of field survey data, which may be interpreted as the layer of highest density of vegetation. It is considered that there are two reasons for this difference. The first reason is the crown shape and maximum canopy height. Since deciduous forest has more even and rounded top canopy, this top canopy might reflect most pulses from LiDAR, which makes it slightly more difficult to penetrate to the layers below. Therefore, the highest canopy cover of deciduous forest, which is also the tallest canopy among the tree forest types<sup>3)</sup>, is detected the most and the highest compared to other forest types.

Second, this difference could be caused by the viewpoint of measurement. Airborne LiDAR detects the vegetation structure from the sky above, which makes it easy to detect the overstory vegetation. However, field survey is conducted above the ground and under the top canopy. The vegetation of lower layers is naturally much easier to

---

3) By Kruskal-Wallis test, it is proved that maximum height and standard deviation of height of three forest types have statistically significant difference both by field and LiDAR data: deciduous forest > mixed forest > coniferous forest (The results of statistics are not shown.).



detect by field survey, making the proportion of relatively lower vegetation layer of dominant trees. Within the layer of overstory (over 5 m), therefore, the proportion of vegetation would show that the lower layer of dominant trees has as much vegetation as the higher layer does.

#### **4. 2. Correlation analysis of vegetation metrics**

Both in the descriptive statistics and correlation analysis, it is evident that the understory vegetation, especially layer 1–2 m, was not generally detected well by LiDAR. This was illustrated in Su & Bork (2007) as well in the description such “cover determination of the understory was impeded by the interception of LiDAR data points by tree overstory.” This similar results are shown in Solberg et al. (2006) as well. Since the height detection of understory by LiDAR was not reliable, so was the cover of understory. They explained this underestimation by 1) declining sampling density of LiDAR by denser overstories, 2) greater DEM error on steep slopes, 3) different plant parts of measurement (field: total plant height vs. LiDAR: sides or ‘shoulder’ of plant canopies) (Su & Bork, 2007). These reasons would be so true in this study as well. Most plots has dense overstories and due to the typical topographical characteristics of Korea slopes of plots were steep<sup>4)</sup>, which might lead to error in the processing DEM.

---

4) The average of slope from field survey was 19.91° (Table 3-1), which is much

Also, since the pulse intensity of LiDAR could be affected by reflectance in plant such as color and continuation of vegetation cover (Su & Bork, 2007), the inherent characteristics of understory in Siheung forest might have been led to less reflectance, making the accuracy of understory detection declined.

However, even in overstory vegetation, the correlation coefficients of layer cover are not as high as those from Su & Bork (2007):  $R^2$  is 0.4070 in layer 5–10 m and  $R^2 = 0.3249$  in layer 10–20 m, whereas  $R^2$  is 0.61 within closed aspen forest in their study. Even though the LiDAR point density employed in this study (3.5 per square meter) is higher than that of Su & Bork (2007) (0.28-1.35 points per square meter), both understory and overstory vegetation showed relatively lower accuracy. The difference on this accuracy on vegetation cover of overstory layer might be attributed from GPS measurement. During the field survey, GPS points was not measured repetitively and the points where the device was placed were not the center of quadrats. Later the GPS point of the center of quadrat was estimated using slopes and aspect. However, LiDAR variables and metrics have been processed in the circular sampling plot based on the GPS measurement from the field. Therefore, if there were greater error on GPS measurement, correlation coefficient between the layer covers would be more insignificant.

---

steeper than the plots of Su & Bork (2007) where the slope gradient was less than 2°.

Martinuzzi et al. (2009) detected understory well with the high accuracy of 83% for classification in the model that they built. In their study, both ground and 1–2.5 m layers was utilized and topography metric such as percent slope multiplied by aspect transformed by cosine was also included in the model. Therefore, in order to acquire more accurate vegetation cover for future studies, 1) the error on GPS should be minimized by repetitive measurement; 2) Models should be constructed considering the Korean forest specific factors such as reflectance of native vegetation and 3) Topographic characteristics, which is represented as steep slopes of many forest areas in Korea should be considered for better detection of understory vegetation cover, as did the study of Martinuzzi et al. (2009).

Unlike understory strata detection by LiDAR, other metrics employed in field survey such as maximum tree height and standard deviation of tree height showed high correlation coefficient values with *hmax* and *std* metrics from LiDAR. Especially *std*, the standard deviation of canopy height correlates not only with standard deviation of tree height from field survey, but also with other site metrics and vertical structure indices. Indeed, the standard deviation of tree height is more indicative of the vertical layering of foliage to characterize vertical element (McElhinny et al. 2005, Zenner, 2000). Therefore it can be said that detecting the standard deviation of canopy height in

a forest with LiDAR will be very effective to identify vertical structure of forest since it is powerful indicative of vertical layering of foliage and easier to extract the values than field survey. Not just for vertical structure of forest, it is an important attribute for structure, meaning that “the forest contains trees with various heights and ages thereby providing a diversity of micro-habitats for wildlife” (Zenner, 2000). It will allow further researches on wildlife habitat in Korea to more easily identify vegetation structure and diversity of habitat. As mentioned above, therefore, building more suited model for identifying understory vegetation cover in Korean forests and utilizing *std* derived from LiDAR which can be utilized as surrogate for other metrics using allometric models will help acquiring precise metrics and variables for wildlife habitat suitability or mapping without surveying in the field only for vegetation.

#### **4. 3. Vegetation structure indices**

Among all vertical structure indices, vertical evenness (VE) classified 4 layers of 0–2 m, 2–5 m, 10–20 m, over 20 m shows the most significant correlation with the same index computed by field survey and other vertical structure indices both from field and LiDAR data. It might be attributed to the combined layer of 2–10 m, which has the highest correlation coefficient of 0.594 (significant at the 0.01 level). However, because it still does not include understory layer of

insignificantly correlated with each other, the difference of the two VE from field and LiDAR data is considered to be high. Those difference was statistically verified by ANOVA (The results are not shown here.) but VE itself has the importance as a vertical structure index for remote sensing using airborne LiDAR since other vertical structure indices does not reflect the actual forest vertical structure without field measurement.

In addition to its usefulness as surrogate, according to the study by Neumann & Starlinger (2001), which originally developed the index of VE, VE also significantly correlated with all indices for horizontal structure used in their study. Those were not able to be computed in this study due to lack of measured metrics from field such as the minimum distance from sample point to nearest tree. However, if VE can be calculated, higher VE by vertically diverse forest structure would be likely mean that it might be a diverse forest horizontally; VE can be a surrogate for horizontal diversity in structure as well.

In VE, low values characterize singlestory forest whereas the maximum value of 1 means vertical equally distributed trees, which is theoretical case. From other researches, VE is being utilized as a metric to verify the vertical structure of different vegetation sites (La Mantina et al. 2008), a stand descriptor for principal component analysis to identify the factor which affect to European larch forest as

disturbance (Garbarino et al. 2009), or a tool to analyze spatial distribution and dynamics of Apennine beech forests with high priority of conservation (Scarnati et al. 2009).

Forests from those study sites have the value of VE as 0.0 to 0.6 for woody forest in a Mediterranean volcanic island (La Mantina et al. 2008), 0.59 to 0.74 for European larch (*Larix decidua* Mill.) forests (Garbarino et al. 2009), and 0.61 to 0.68 for mean value of Apennine beech forests (*Taxus baccata* & *Ilex aquifolium*, Scarnati et al. 2009).

Even though the mean VE values from two data source is statistically different by ANOVA, VE computed by LiDAR data can discriminate the three forest types. The p-value for this discrimination is 0.009 and deciduous and coniferous forest can be statistically separate in the p-value of 0.010. No vertical structure indices can differentiate the forest type by ANOVA but since the correlation between field and LiDAR data is significant, VE also can utilized to differentiate forest type by data derived from airborne LiDAR as well as the degree of evenness in vertical structure of forest.

Although VDR (Goetz et al. 2007) was calculable by only LiDAR metrics, it shows significant correlation with other vertical structure indices from field measurements, explaining that this index can be utilized as an indicative of future studies to identify vertical structure

of Korean forest using airborne LiDAR data. Originally VDR was designed to figure out the correlation with bird species richness with full waveform LiDAR, so the results of this study shows that the application of VDR will further reach to various ecological studies which deals with both avian community and vegetation as habitats with discrete pulse LiDAR.

On the contrary to the results of the study by Neumann & Starlinger (2001), in which vegetation structure indices insignificantly correlate with species diversity indices, this study figure out that tree species indices such as RI, SH, SI and EI with tree number have significant correlation with vertical structural indices from LiDAR metrics. This can be interpreted as indices like FHD with Shannon index or VE from LiDAR not only present high diversity in vertical structure of forest but also suggest that the forest would have high tree species diversity and evenness as well. Note that the VE with 6 layers shows higher correlation coefficient with tree species indices than VE with 4 layers, which were one of the best indices to measure vertical structure by LiDAR metrics.

## 5. Conclusions

With data derived from LiDAR and field survey on forests in Siheung city, these below were identified:

- 1) The accuracy of LiDAR data was not as significantly high as what one presumes, especially in understory strata of 1–2 m. Nevertheless, the proportion of the vegetation cover by layer from LiDAR data depicts and separates three different forest types with curves of cover graphs by layers.
- 2) To acquire more accurate vegetation cover for future studies, i) the error on GPS should be minimized by repetitive measurement; ii) Models should be constructed, which consider the Korean forest specific factors such as reflectance of native vegetation and iii) Topographic characteristics, which is represented as steep slopes of many forest areas in Korea should be considered for better detection of understory vegetation cover, as did the study of Martinuzzi et al. (2009).
- 3) The direct metric such as the standard deviation of canopy height from LiDAR data can be used as good indicative of vertical structure of vegetation in the simplest and the most efficient way.
- 4) Vertical structure indices such as vertical evenness (VE) and



vertical distribution ratio (VDR) computed from LiDAR data effectively explain the diversity of vertical structure with significant correlation with indices from field data, which allows to apply to future studies upon vertical structure of vegetation. Also VE from LiDAR data could differentiate forest types and have fairly significant correlation with other indices such as tree species indices, proving that above-mentioned discoveries on VE can be the most suitable index to identify vertical structure using discrete pulse airborne LiDAR.

However, since the first correlation between the data on the proportion of cover does not show highly significant correlation between LiDAR and field survey metrics, methods on improving the accuracy and effectively detecting understory vegetation with LiDAR for the future studies are critically essential.

## **Acknowledgement**

This study was supported by the National Research Foundation of Korea (NRF) grant funded by the Ministry of Education, Science Technology (No. 2011-0024289 and No. 2012-0008361).

## **<References>**

- Ambuel, B., and S. A. Temple.(1983) “Area-Dependent Changes in the Bird Communities and Vegetation of Southern Wisconsin”, *Ecology*, 64(5):1057-1068.
- Baltsavias, E. P.(1999), “Airborne laser scanning:basic relations and formulas”, *ISPRS Journal of Photogrammetry and Remote Sensing*, 54: 199–214.
- Buongiorno, J., S. Dahir, H. Lu, C. Lin.(1994) “Tree Size Diversity and Economic Returns in Uneven-Aged Forest Stands”, *Forest Science*, 40(1):83-103.
- Clifford, H. T. and W. Stephenson.(1975), An introduction to numerical classification, Academic Press, New York.
- Falkowski, M. J., J. S. Evans, S. Martinuzzi, P. E. Gessler, and A. T. Hudak.(2009), “Characterizing forest succession with lidar data: An evaluation for the Inland Northwest, USA”, *Remote Sensing of*

- Environment*, 113(5): 946-956.
- Garbarino, M., P. J. Weisberg, R. Motta.(2009), "Interacting effects of physical environment and anthropogenic disturbances on the structure of European larch (*Larix decidua* Mill.) forests", *Forest Ecology and Management*, 257 (2009): 1794 - 1802.
- Goetz, S., D. Steinberg, R. Dubayah, and B. Blair.(2007), "Laser remote sensing of canopy habitat heterogeneity as a predictor of bird species richness in an eastern temperate forest, USA", *Remote Sensing of Environment*, 108:254 - 263.
- Helmer, E. H., T. S. Ruzyski, J. M. Wunderle Jr, S. Vogesser, B. Ruefenacht, C. Kwit, T. J. Brandeis, and D. N. Ewert.(2010), "Mapping tropical dry forest height, foliage height profiles and disturbance type and age with a time series of cloud-cleared Landsat and ALI image mosaics to characterize avian habitat", *Remote Sensing of Environment*, 114(11), 2457-2473.
- Holdridge, L.R., 1967. Life zone ecology. Tropical Science Center, San Jose, Costa Rica.
- IBM Corp.(2011) IBM SPSS Statistics for Windows, Version 20.0. Armonk, NY: IBM Corp.
- Karr, J.(1968) "Habitat and Avian Diversity on Strip-Mined Land in East-Central Illinois", *The Condor*, 70(4):348-357.
- KICT.(2009), "Final report upon production of secondary biotope map of Siheung", Korea Institute of Construction Technology, Siheung City.
- KIST.(2005), "항공 LiDAR를 이용한 산림측정 기술의 개요 및 연구 동

향”, KIST.

Kim, E., G. Wie, H. Cho, and L. Yang.(2010), “A Study for Forest Research using Airborne Laser Scanning”, *Journal of the Korean Society of Surveying, Geodesy, Photogrammetry, and Cartography*, 28(3): 299-304.

Latham, P. A., H. R. Zuurig, and D. W. Coble.(1998), “A method for quantifying vertical forest structure”, *Forest Ecology and Management*, 104: 157-170.

La Mantina, T., S. Ruhl, D. Pasta, D. G.Campisi, and G. Terrazzino.(2008) “Structural analysis of woody species in Mediterranean old fields”, *Plant Biosystems*, 142(3): 462-471.

Lee, K., and C. Lee.(2005), *Outline and Research Trend of Forest Measurement Technology using Airborne LiDAR*, KIST.

Lee, S., B. Lee, J. Kim, and C. Kim.(2009), “Accuracy Evaluation of LiDAR Measurement on Forest Area”, *Journal of the Korean Society of Surveying, Geodesy, Photogrammetry, and Cartography*, 27(5): 545-553.

Lloyd, M., and R. J. Ghelardi.(1964), “A table for calculating the "equitability" component of species diversity”, *Journal of Animal Ecology*, 33:217-225.

MacArthur, R., H., and J. W. MacArthur.(1961), “On Bird Species Diversity”, *Ecology*, 42(3): 594-598.

Magurran, A.E.(1988), *Ecological Diversity and its Measurement*. Princeton University Press, New Jersey.

- Martinuzzi, S., L. A. Vierling, W. A. Gould, M. J. Falkowski, J. S. Evans, A. T. Hudak, and K. T. Vierling.(2009), "Mapping snags and understory shrubs for a LiDAR-based assessment of wildlife habitat suitability", *Remote Sensing of Environment*, 113(12): 2533-2546.
- McElhinny, C., P. Gibbons, C. Brack, J. Bauhus.(2005), "Forest and woodland stand structural complexity: Its definition and measurement", *Forest Ecology and Management*, 218:1-24.
- McElhinny, C., P. Gibbons, C. Brack.(2006), "An objective and quantitative methodology for constructing an index of stand structural complexity", *Forest Ecology and Management*, 235:54 - 71.
- Neumann, M. & F. Starlinger.(2001), "The significance of different indices for stand structure and diversity in forests", *Forest Ecology and Management*, 145: 91-106.
- Optech Incorporated.(2003) "ALTM 3070 Datasheet",  
[http://www.optech.ca/pdf/Specs/specs\\_altm\\_3070.pdf](http://www.optech.ca/pdf/Specs/specs_altm_3070.pdf),
- R Development Core Team.(2011), R: A language and environment for statistical computing. Vienna, Austria: R Foundation for Statistical Computing, ISBN 3-900051-07-0, <http://www.R-project.org/>.
- Roth, R.(1976), "Spatial Heterogeneity and Bird Species Diversity", *Ecology*, 57(4):773-782.
- Ryu, J.(2010), Diversity assessment of forest structure to improve biodiversity, Master's Dissertation, Seoul National University.
- Scarnati, L., F. Attorre, M. De Sanctis, A. Farcomeni, F. Francesconi, M.

- Mancini, and F. Bruno.(2009), “A multiple approach for the evaluation of the spatial distribution and dynamics of a forest habitat: the case of Apennine beech forests with *Taxus baccata* and *Ilex aquifolium*”, *Biodiversity Conservation*, 18:3099–3113.
- Schemske, D. W., and N. Brokaw.(1981), “Treefalls and the Distribution of Understory Birds in a Tropical Forest”, *Ecology*, 62(4), 938-945.
- Siheung City (2011), “Statistics of land cadastre in Siheung”, December 2011, Siheung City.
- Simpson, E.H.(1949), “Measurement of diversity”. *Nature* 163:688.
- Solberg, S., E. Naesset, and O. M. Bollandsas.(2006), “Single Tree Segmentation Using Airborne Laser Scanner Data in a Structurally Heterogeneous Spruce Forest”, *Photogrammetric Engineering & Remote Sensing*, 72(12):1369–1378.
- Sullivan, T. P., D. S. Sullivan and P. M. F. Lindgren.(2001), “Stand Structure and Small Mammals in Young Lodgepole Pine Forest: 10-Year Results after Thinning”, *Ecological Applications*, 11(4):1151-1173
- Su, J. G., and E. W. Bork..(2007), "Characterization of diverse plant communities in Aspen Parkland rangeland using LiDAR data", *Applied Vegetation Science* 10:407-416.
- Vierling, K. T., L. A. Vierling, W. A. Gould, S. Martinuzzi, and R. M. Clawges.(2008), “Lidar: shedding new light on habitat characterization

and modeling”, *Frontiers in Ecology and the Environment*, 6(2): 90-98.

Yoon, E., and I. Lee.(2000), “Development of Satellite Image Classification Method for the Analysis of vegetation Structure”, *Proceedings of Korean Society of Environment & Ecology Conference* 1: 87-90.

Yoon, J., K. Lee, J. Shin, and C. Woo.(2006), “Characteristics of Airborne Lidar Data and Ground Points Separation in Forested Area”, *Journal of Korean Society of Remote Sensing*, 22(6): 533-542.

Zenner, E. K.(2005), “Investigating scale-dependent stand heterogeneity with structure-area-curves”, *Forest Ecology and Management*, 209(3): 87-100.

Zenner, E. K. and D. E. Hibbs.(2000), “A new method for modeling the heterogeneity of forest structure”, *Forest Ecology and Management*, 129: 75-87.

국문초록

# LiDAR 데이터를 이용한 식생 지수 개발과 시흥시 산림 수직 구조 분석

조 선

서울대학교 환경대학원 환경계획학과

2013 년 2 월

지도교수 이도원

서식지로서 식생구조는 야생동물들의 다양성과 풍부도에 영향을 미친다. 이 구조를 밝히기 위한 원격탐사 기법은 생태학과 산림학 분야에서 나날이 발전해 왔다. 본 논문은 3차원의 정보를 획득하는 원격탐사 기술 중 하나인 항공 LiDAR (Light Detection And Ranging)를 이용하여 산림의 식생구조를 정확히 밝힐 수 있는 식생 구조 지수를 개발하는 것을 목적으로 하고 있다. 시흥시의 산림을 대상으로 LiDAR의 비지면 리턴 (non-ground return)을 이용하여 식생의 피도 데이터를 여섯 층으로 나누어 수직구조 데이터를 구축하였다. 이를 현장조사와 결과와 비교하여 시흥시 내 비교적 뚜렷한 세 가지 산림 유형의 특징을 구별하였다. 또한 LiDAR에서 도출된 식생의 층별 피도값과 수고값을 다양한 식생 수직 구조 지수에 대입하여 각 사이트의 식생 수직 구조 지수를 구축하였다. 수고 및 층별 피도, 목본의 수 등과 같은 현장 조사 데이터를 이용해 구축한 식생 수직구조 지수, 목본의 종 다양성 지수, 목본의 생체량 지수 등과 같은 다른 지수들을 이용해 LiDAR로부터 도출된 지수와의 상관성을 분석하였다. 이 분석을 통하여 수직 균등도 지수 (vertical evenness index, VE)가 현장



조사에서 얻어진 VE의 값과 가장 상관이 높은 것으로 밝혀졌다. 또한 통계 분석의 결과, LiDAR 데이터에서 도출된 VE는 시흥시의 세 가지 산림 유형을 유의미하게 구별할 수 있었으며, 현장에서 조사된 목본의 종 다양성 지수와도 높은 상관을 보임으로써 수직구조지수를 통한 다양한 식생구조의 특징과 유형을 알아낼 수 있음을 시사하였다. 비록 GPS측정의 오차 및 하층식생의 피도가 정확하게 측정되지 못한 것으로 인하여 전체적인 LiDAR의 정확도는 다른 연구에서 예측한 것만큼 높지는 않았으나, 이러한 한계점은 다음과 같은 방법으로 개선될 수 있을 것으로 생각된다. 오차를 최소화하고 상층과 하층 모두의 정확한 측정값을 획득하기 위해서는 반복적인 GPS의 측정과 보정을 통하여 그 오차를 줄이고, LiDAR 펄스의 반사도나 파동의 강도에 영향을 미칠 수 있는 한반도 고유 식생 및 지형에서 나타나는 요인들을 잘 분석하여 모델에 반영해야 할 것이다. 이러한 방법을 통하여 정확한 LiDAR 데이터를 구축하고, 본 연구에서 통계적으로 입증된 식생 구조 지수들을 잘 활용한다면, 추후 이산적 (discrete) 항공 LiDAR를 이용하여 야생동물들의 서식지로서의 식생 구조를 분석하는 연구에 도움이 될 것으로 사료된다.

**주요어 :** 산림 수직 구조, 식생 지수, 항공 LiDAR, 시흥시

**학 번 :** 2010-23897